Surface Imaging for Patient Setup and Monitoring for Breast Radiotherapy

By

Lynn Novella Book

B.S. Nuclear Engineering (2005)
University of Illinois, Champaign-Urbana

Submitted to the Department of Nuclear Science and Engineering
In Partial Fulfillment of the Requirements for the Degree of
Master of Science in Nuclear Science and Engineering

At the

Massachusetts Institute of Technology

January 2007
[February 2007]

Signature of Author_____
Department of Nuclear Science and Engineering
January 2007

Certified by_____
David P. Gierga
Radiation Physicist, Massachusetts General Hospital
Instructor in Radiation Oncology, Harvard Medical School
Thesis Supervisor

Certified by_____
Jeffrey A. Coderre
Associate Professor of Nuclear Science and Engineering
Thesis Co-Supervisor

Accepted by_____
Jeffrey A. Coderre
Chairman, Department Committee on Graduate Students

Surface Imaging for Patient Setup and Monitoring for Breast Radiotherapy

By

Lynn Novella Book

Submitted to the Department of Nuclear Science and Engineering
On January 12, 2007 in Partial Fulfillment of the
Requirements for the Degree of Master of Science in
Nuclear Science and Engineering

ABSTRACT

Approximately one in eight women will get breast cancer at some point in their lives. A promising new treatment is partial breast irradiation, in which multiple radiation beams cross at the tumor site within the patient. This method of radiotherapy treats only a portion of the breast for a relatively small number of treatments with a high dose per treatment. This method requires much higher accuracy of patient alignment as the tumor site must be correct targeted. This study examined the possibility of using the VisionRT (London, UK) software and cameras for surface visualization to align patients for this treatment. A portable, single pod, the "Mini Cam" was found to be able to generate images for translations less than 2.5-5.5 cm, depending on the direction of translation. Calibration was a key aspect to ensuring accurate results. Eight patients were studied for deformation, breathing motion and day to day alignment. Surface images were taken at several points during regular treatment. Deformation was found to be small and never exceeded and average value of 2 mm. No correlation was found between the amount of deformation and the breast size or planning treatment volume. The average peak-to-peak breathing motion was 0.99-2.16 mm. Variability was discovered in the gating function of the VisionRT software. Aligning patients based on the first treatment session was found to be more accurate than aligning to a CT image taken weeks earlier.

Thesis Supervisor: David P. Gierga
Title: Radiation Physicist, Massachusetts General Hospital and Instructor in Radiation Oncology, Harvard Medical School

Table of Contents

Tables:

Figures:

I. Background

1. Breast Cancer Treatments

Currently there are several methods to treat breast cancer, including surgery, radiation therapy, chemotherapy and hormone therapy. Breast cancer is currently estimated to occur in one in eight women (1). One common treatment consists of surgery to remove the tumor followed by radiation therapy to the whole breast. The number of women who are candidates for radiation therapy varies strongly with the stage of the disease. Anywhere from 10-70 % of those candidates receive radiation therapy (2). Factors against radiation therapy for candidates are often logistical. For example daily radiation therapy is difficult for the elderly or those living far away from a clinic to attend. Conventional radiation therapy consists of several radiation beams aimed at the tumor site. The beams target the tumor from different angles in an effort to spare healthy tissue. Since the planning target volume (PTV) usually encompasses the entire breast being treated, this method is less sensitive with respect to patient setup error. As the whole breast is treated, small errors in patient alignment do not move the tumor out of the treatment area. Conversely, this means that more healthy tissue surrounding the tumor is exposed to high level of radiation, which could cause significant damage. In conventional, whole breast irradiation it is advised that less than 60 percent of the breast receive more than 50 percent of the prescribed radiation dose. Less than 35 percent of the breast is advised to receive the full radiation dose (3).

2. Partial Breast Irradiation

Within the field of radiation for breast cancer, there is a new group of techniques called partial breast irradiation (PBI). These techniques were devised in order to spare more normal, healthy tissue, while delivering a higher dose to the tumor, compared with conventional whole breast external beam radiation. The procedure exposes only the area of the breast containing the lumpectomy site to the therapeutic radiation. This reduces the radiation damage to the healthy tissue surrounding the tumor site. This method also allows for a shorter treatment schedule. PBI is still undergoing clinical trials, in part to study if PBI provides the same or better tumor local control as whole breast irradiation (4). There are several methods of PBI to be considered.

Brachytherapy is the one type of PBI, consisting of two popular methods. One method uses the MammoSite balloon catheter. The MammoSite approach involves the surgeon inserting a balloon with a catheter into the void left by a lumpectomy and inflating it with saline (5). During treatment a wire with a radioactive seed, usually Ir-192, is inserted into the void, via the catheter. This gives a radiation dose directly to the lumpectomy site. The second method, interstitial brachytherapy, uses multiple catheters around the tumor site (5). During treatment, wires with radioactive seeds are inserted into each catheter to deliver radiation.

The second type of PBI considered here is external beam radiation PBI. The sparing of healthy tissue, while delivering a full dose to only the tumor site, is achieved by the careful planning of the radiation beams. The beams are directed at the patient such that the beams will cross at the site of the tumor, giving a combined dose to the tumor,

but only a single beam dose to healthy tissue. Accuracy in patient setup is paramount as the tumor must be at the exact spot the radiation beams cross to receive the full dose.

In this method, the PTV consists of just the region surrounding the lumpectomy site, as opposed to the entire breast that conventional methods treat. As this method only targets the tumor, doses can be given in higher amounts and with more frequency. This means that the cancerous cells have less time to regenerate between treatments, while still sparing healthy tissue. The typical whole breast treatment consists of 25-30 fractions (one per weekday) of 2 Gy each, while PBI (according to the current Massachusetts General Hospital protocol) consists of 9 fractions (2 per weekday) of 4 Gy. This is an effective method to target only the tumor, but requires a much higher level of accuracy than conventional radiation treatments.

3. Patient Alignment

This need for greater accuracy has spurred advances in patient setup for treatment. There are five methods, in various stages of clinical use, to align patients for partial breast irradiation. The five methods are lasers, chest wall alignment, clips, cone beam CT and surface visualization.

a. Lasers

The most convention method of patient alignment has been lasers and skin tattoos. In this method a patient is given a small tattoo in a specific spot(s) at the time of CT simulation. In future treatments the patient can be setup accurately by lining up the tattoos with lasers. This method is often used because it is reasonably accurate, cost

effective and non-invasive. The main concern with this method is that the accuracy is not high enough for use in PBI. One major problem arises if the arm is in a different position, the skin may be moved relative to the tumor. The elasticity of the skin is a source of error in these setups. The error is likely negligible when doing whole breast irradiation, but becomes significant with the additional accuracy needed for PBI.

b. Chest Wall Alignment

Another common method is looking at the chest wall, via x-rays. The radiation therapist can compare x-rays from an initial session to one taken for the current treatment and use them to place the patient in the same position as when the first x-ray was taken. This method is often used in addition to laser setup as a way to improve patient setup accuracy. The main concern is that the placement of the breast tissue/tumor does not necessarily directly correspond to the location of the chest wall.

c. Clips

The third method used is by looking at metal clips. After a lumpectomy, the surgeon will place several small metal clips at the site before closing up. These radio-opaque metal clips can then be used as reference points, at the tumor site, to line up the patient for treatment (6). The clips are easily viewed via x-ray. This method is more reliable than the first two methods due to the fact that the reference points are at the tumor site, so changes in the location of the tumor when compared to the skin or chest wall are not reasons for concern. One problem at this point is possible movement of the clips. It is not yet known if clips placed at the site of the lumpectomy are subject to

migration within the tumor area. Another problem with this method is the possible reluctance of surgeons to leave the clips at the lumpectomy site.

d. Cone Beam CT

Cone beam CT is a new technique in external beam radiotherapy. It consists of radiation in a cone shape, which is rotated about a patient, with images taken every few degrees. The images can then be reconstructed into a 3D volume. As the cone beam images an entire volume at once, instead of slices, the resolution is much higher (7-9). This allows physicians to more accurately plan radiation treatments and align the patients for those treatments. The main concern regarding this method is the additional radiation exposure to patients, especially considering the sensitive nature of the breast tissue. For example, to get the same image quality from a 32 cm body phantom, a single slice helical CT scan will deliver a 0.015 Gy dose to the isocenter and a 0.025 Gy dose to the skin while a cone beam scan will deliver a 0.028 Gy dose to the isocenter and a 0.044 Gy dose to the skin (10). This method is still being developed and is not yet in widespread use in breast cancer radiotherapy.

e. Surface Visualization

The final method is surface visualization and looks at a 3D surface image of the patient using a system of 4 cameras located in two "pods" mounted to the ceiling (11-12). A program called AlignRT (VisionRT London, UK) is used to image the patient and has the ability to align the new image to a past image and tell the therapist how much and in what direction the couch should be moved to correctly align the patient for treatment. The program allows for couches with four or six degrees of freedom (3 directions of

translation and one or three directions of rotation). The major concerns are whether or not there is any deformation in the breast over the course of treatments that could cause erroneous results, whether the surface of the breast accurately correlates with the tumor site and whether breathing will affect the alignment results. Deformation is potentially significant when looking a soft tissue such as the breast because if the skin's surface deforms, it may cause the lumpectomy site to shift as well. Breathing deeply could cause all or part of the tumor site to shift out of the PTV which would mean the wrong volume is being treated. PBI is promising though, because it allows for patient setup and real-time monitoring without exposing the patient to additional radiation.

4. Motivation

This research will examine three questions. First, it is important to examine the deformation that may occur over the course of treatment in order to determine if it poses a significant problem for aligning patients. Second, this research will study the effects of breathing on patient alignment. It is important to know how much movement of the surface is caused by breathing. Finally a comparison between the clip and surface alignment will be done. Assuming that clip placement is the gold standard for alignment, this research will demonstrate the accuracy of the surface alignment. This will provide an assessment of the correlation of the skin surface to the tumor site.

II. Materials

1. VisionRT Camera System

The 3D alignments in this research were found using the AlignRT (VisionRT, London, UK) camera system and associated computer software (13). This technology consists of two "pods" of cameras, each containing 2 data cameras, speckle projector, flash and a texture camera. Figure 1 shows one of the two pods of cameras mounted on the ceiling in the treatment room.

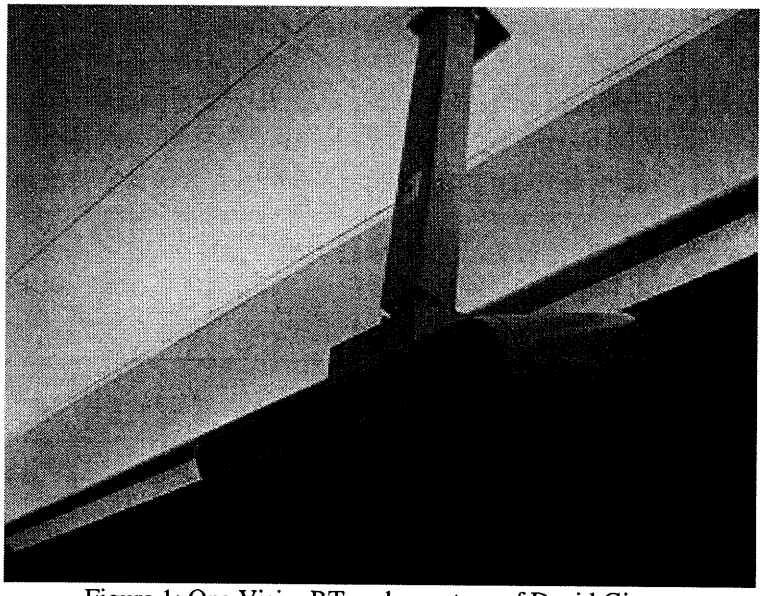

Figure 1: One VisionRT pod, courtesy of David Gierga

Each pod can function independently, but using both pods will allow a greater field of view. In order to obtain the 3D surfaces, each pod projects a pseudo-random speckle pattern onto the patient. This makes each point on the patient unique to AlignRT and allows for triangulation by the program to determine the exact distance away of each point on the patient. Compiling all of the known distances together creates the 3D surface data. Each pod captures data over 120 degrees axially (11).

Figure 2: Example surface image.

Among its many features, the AlignRT software is able to display and store this 3D data. Figure 2 demonstrates a typical surface created by the AlignRT program. The program is able to compare images to previously taken images and align them with accuracy better than 0.8 mm and 0.1° rms (12).

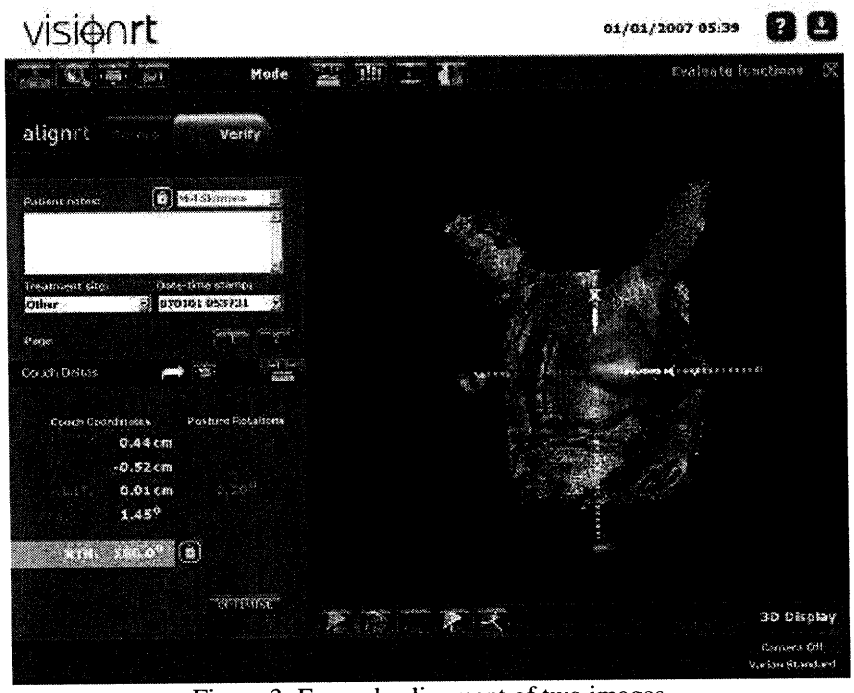

Figure 3: Example alignment of two images.

The program compares two 3D images with or without a region of interest specified, and calculates the translations or rotations required to best align the surfaces. Figure 3 shows the resulting alignment when comparing two images. It shows the recommended shifts as well as an overlay of the two images, based on the best fit of the region of interest. Figure 4 demonstrates the ability of the program to select the region of interest.

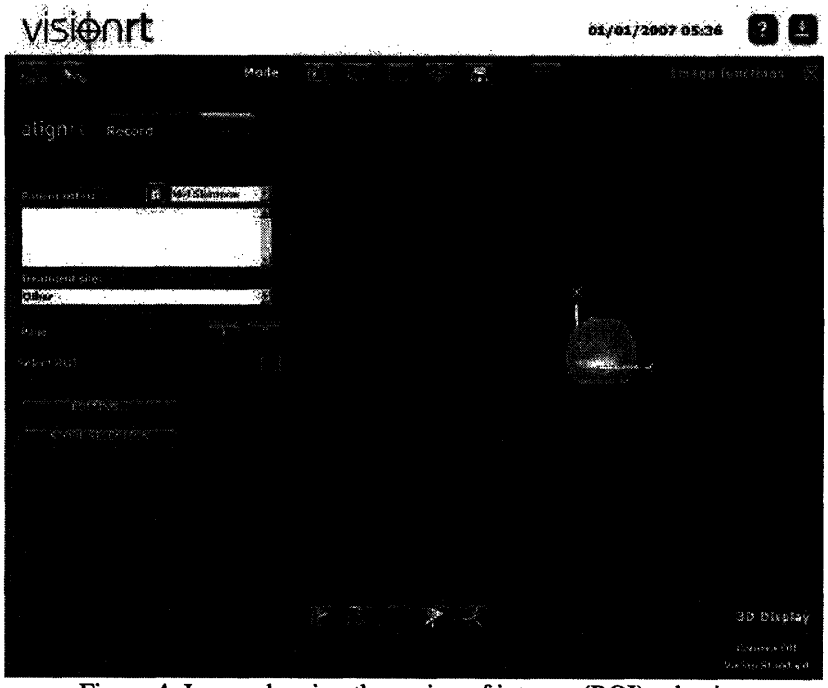

Figure 4: Image showing the region of interest (ROI) selection

The software can also be used to monitor patients or even record a short movie (10 seconds) of the surface data. This is ideal for use in a breathing analysis. This gating function takes a series of images (7.5 per second). The user selects a point on the surface and then the program creates a trace, marking the vertical movement in millimeters. Figure 5 shows an example trace of a single point on the patient's breast. The trace is normalized for the lowest (exhale) point and varies from 0 to 1.9 mm.

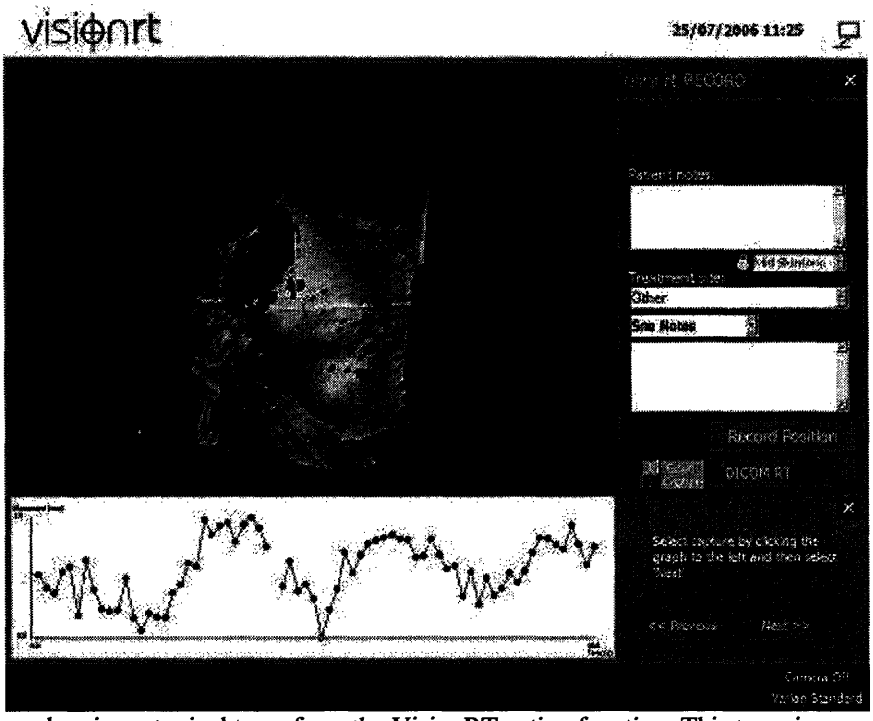

Figure 5: Image showing a typical trace from the VisionRT gating function. This trace is normalized for the lowest value in the sample and varies from 0 to 1.9 mm.

The isocenter (or as close as possible) was chosen so the results would mimic the movement of the tumor site as much as possible. The isocenter is defined as the center of the tumor site to be treated. The trace was automatically re-normalized so that the lowest level (exhale) was at zero millimeters. This image number was termed the reference image. The program then allowed the user to pick any point on the trace and extract the 3D image data for that point.

2. Visualization Toolkit

The Visualization Toolkit (VTK), of Kitware Inc., is a freeware system that has been used to write a C++ program, written by Marco Riboldi, to analyze the match up between two surfaces (11, 14). The program takes an input of two surfaces with the option of a region of interest selection and produces a text file listing the distance between the surfaces for each point respectively and a color wash image which visually

represents the distance between the surfaces. The image is color coded to illustrate the separations: green for distances within ±2 mm, blue for ±2-4 mm, red for ±4-6 mm and gray for outside of ±6mm.

3. On-Board Imaging

On-board imaging, OBI, (Varian Medical Systems) is a kilovoltage x-ray combined with computer software that allows alignment and visualization of the tumor site (16). The machine allows for 3 degrees of freedom for imaging the tumor site. The therapist has the OBI take both a lateral and an AP x-ray of the patient for alignment purposes. For this study, all images were taken at exhale. The software then allows the therapist to find the shifts needed to align the patient. This is done by comparing the x-rays taken by the OBI with digitally reconstructed radiographs (DRR) created from the CT scan taken 1-2 weeks before radiation treatment had begun. The DRR image is the expected treatment position of the patient. This alignment is done by having the therapist match the location of the clips at the tumor site in both images. The OBI system then calculates the recommended couch shift to correctly align the patient and robotically completes the shift. Figure 6 shows the linear accelerator/OBI system and sample x-ray images taken by OBI.

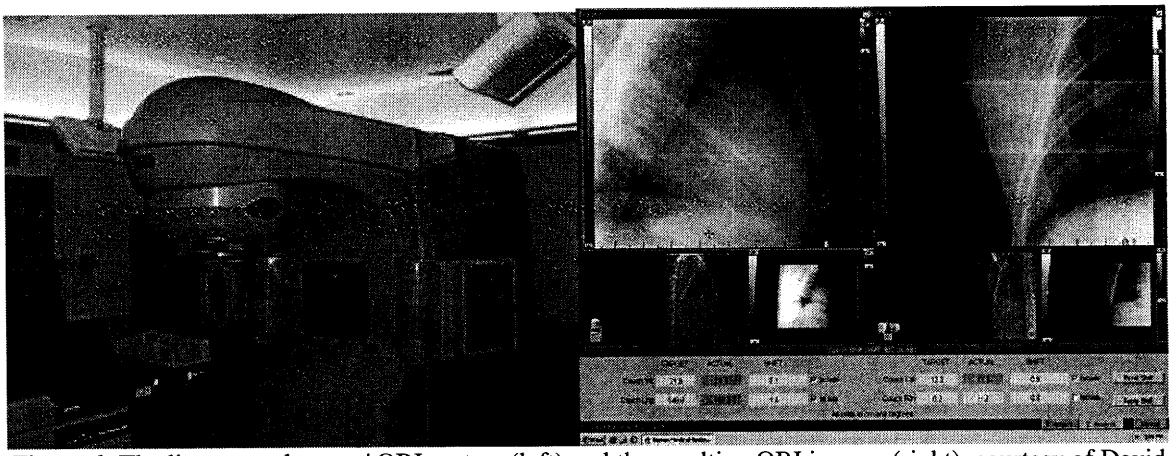

Figure 6: The linear accelerator / OBI system (left) and the resulting OBI images (right), courtesy of David Gierga.

4. Treatment Sequence

The patients in this study all underwent a similar procedure for radiotherapy. First they had lumpectomy surgery to remove the tumor mass. At this time, the surgeon also placed several radio opaque clips at the site to help identify the location in the future. When the patient was scheduled to begin radiotherapy, they first had a CT scan. From this scan, radiographs could be digitally reconstructed for use as a reference surface by the OBI system and a surface could be reconstructed for use by the AlignRT program. The radiotherapy treatment plan is also devised based on the CT scan. One to two weeks after the CT scan, radiation treatments began. Each patient was given 8-9 fractions, in 2 sessions per day and over 4-5 days. At the first session, the patient was aligned via lasers initially and then corrected by the OBI system. A surface image was taken after the patient had been aligned by lasers and then after they were realigned by the OBI.

III. Mini Cam Analysis

1. Methods

The Mini Cam is a portable version of the AlignRT camera system, consisting of one pod of 2 cameras. It has many possible applications such as patient alignment during proton therapy or as a method to view how well a dural plaque is molding to the spine in vertebral or paravertebral tumor resections (15). In an effort to characterize the Mini Cam, a series of experiments were run by moving the camera in one of 4 directions, vertical (VRT), latitude (LAT), longitude (LNG) or rotation about the vertical axis (ROT), by a known amount and recorded the couch translations recommended by AlignRT. The AlignRT program does allow for a possible 6 degrees of freedom by adding rotation about the latitude (RLAT) and longitudinal (RLNG) axes. A spine phantom, set on a mechanical stage, was imaged (Figure 7).

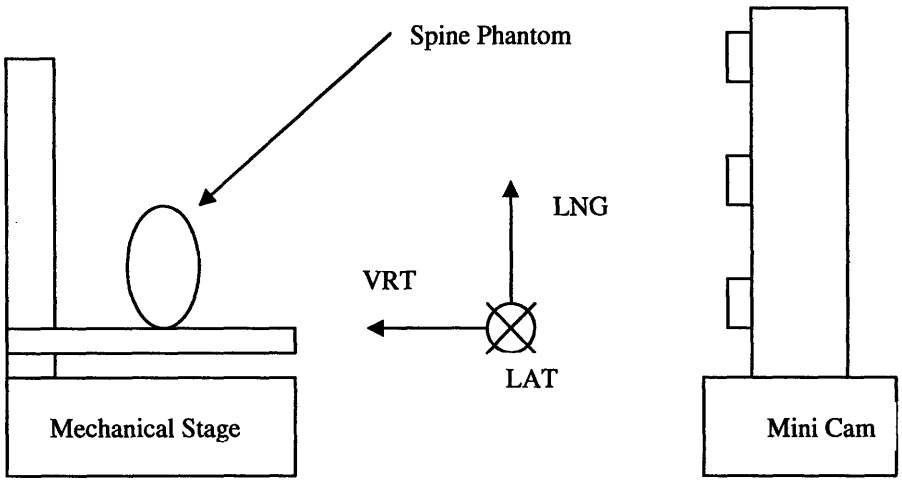

Figure 7: Setup of Mini Cam with relation to mechanical stage.

The mechanical stage allowed six degrees of freedom and has a precision of 1/100 mm. The phantom was set up at the focal point of the camera, 0.9 m, as determined by calibration, making this point the "zero" point, or origin of the system. An AlignRT surface image was recorded at the origin. The stage was then moved a known amount, in

either the vertical, latitude, longitude or rotation (about the vertical axis) direction. Another surface image was taken at the new location. The AlignRT program was then run, aligning the surface it had recorded at the origin to the surface recorded after a known movement. The resulting shifts gave the amount that the AlignRT program thought the phantom had been moved.

A simple analysis was performed comparing the known movement with the suggested movement. The calibration of the Mini Cam was accomplished with a special calibration plate at the focal distance of the camera. The plate is printed with many equally spaced black dots with 4 larger markers among the dots (Figure 8).

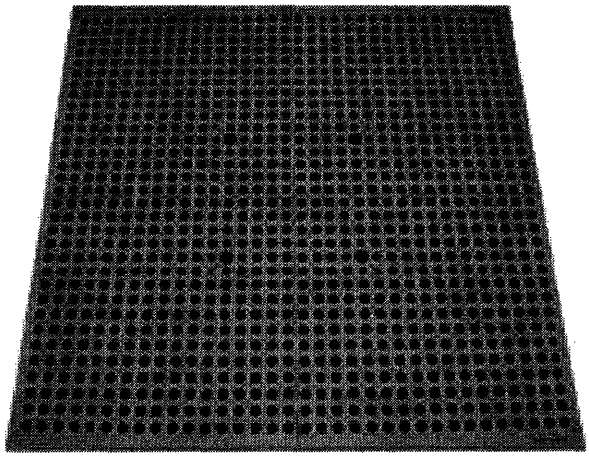

Figure 8: Image showing the calibration plate used in AlignRT. The Mini Cam uses a smaller version. (13)

During calibration, the camera images the plate and the user is asked to select the location of the 4 large markers on the image. The location of the markers with respect to the dots is exactly known to the program, so to demonstrate calibration has been successful, it marks all of the black dots within the image. If the computer incorrectly marks the dots, the calibration has been unsuccessful. The calibration sets the internal axes and the focal point of the camera. The internal axes are set by the exact location and

angle of the calibration plate. For example, vertical is always the direction perpendicular to the plate. This calibration method allows the camera to be calibrated in one location and moved to another to take images.

Finally, the field of view was found for the camera. This was achieved by placing the spine phantom at the focal point of the camera and shifting the phantom vertically and horizontally until the phantom was no longer imaged completely.

2. Results

The results demonstrated a definite correspondence to the correct direction of motion, meaning that the mini-cam accurately measured the phantom movement. This is shown (Figure 9) in how close the line of interest in each graph is to the identity line. Figure 9 shows the resulting motions recorded by the computer when the phantom was moved in a single direction. As the resulting motions are 3 translations in mm and 3 rotations in degrees, the axes reads in both mm and degrees. The data is combined to show trends, but in not directly comparable due to the differing units. In every graph, a slight drift can also be seen for most of the other possible degrees of freedom, even though the phantom has not been moved in these directions. The possible reasons for this are discussed later.

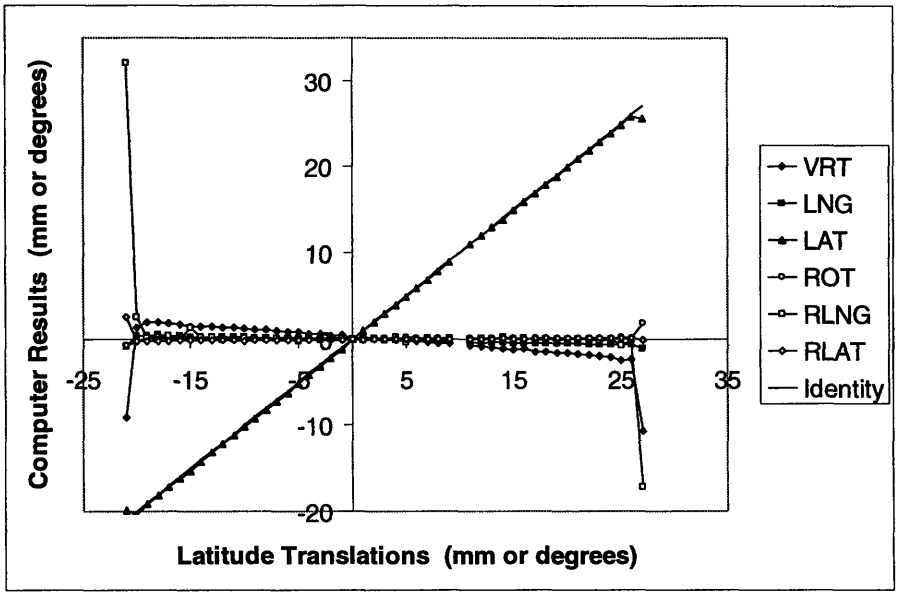
Computer Results (mm or degrees)
30
20
10
-10
-20
-25
-15
5
15
25
35
Latitude Translations (mm or degrees)
VRT
LNG
LAT
ROT
RLNG
RLAT
Identity

9a

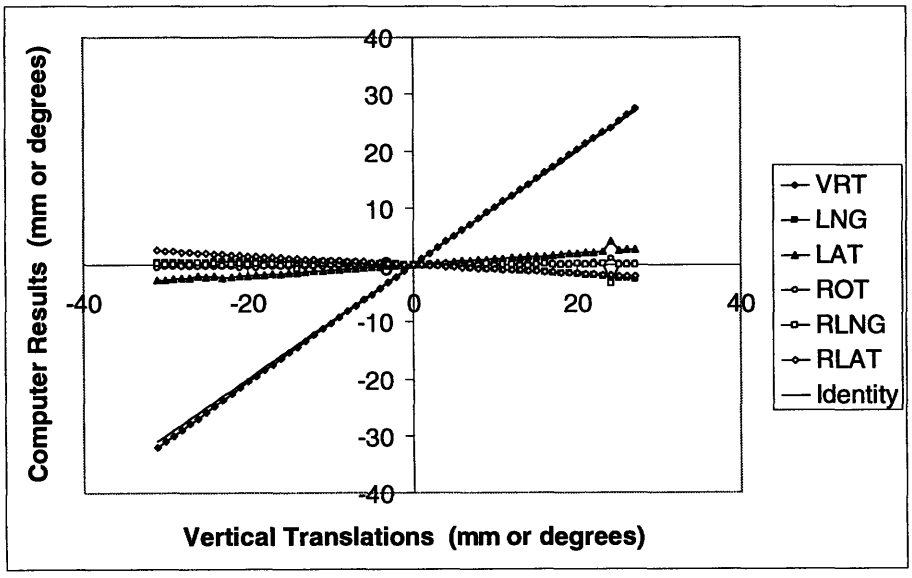
Computer Results (mm or degrees)
40
30
20
10
-10
-20
-30
-40
-40
-20
0
20
40
Vertical Translations (mm or degrees)
VRT
LNG
LAT
ROT
RLNG
RLAT
Identity

9b

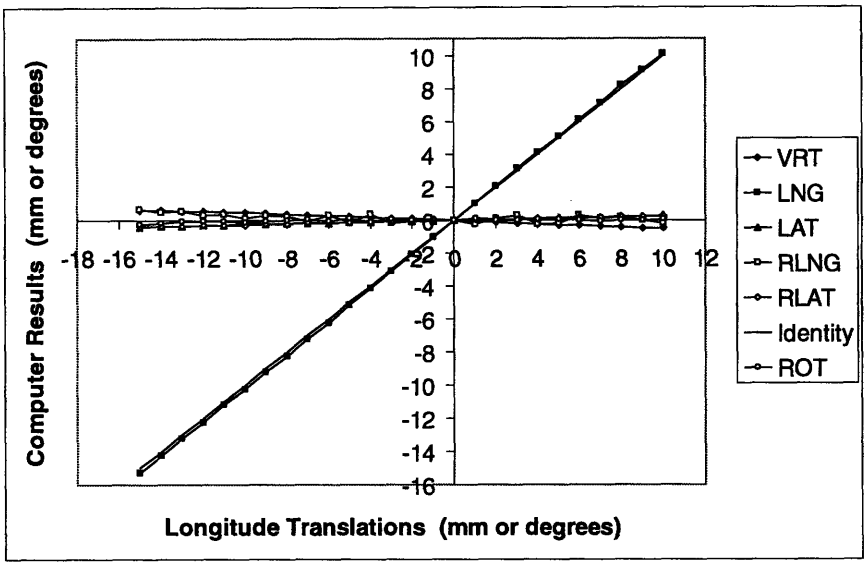

9c

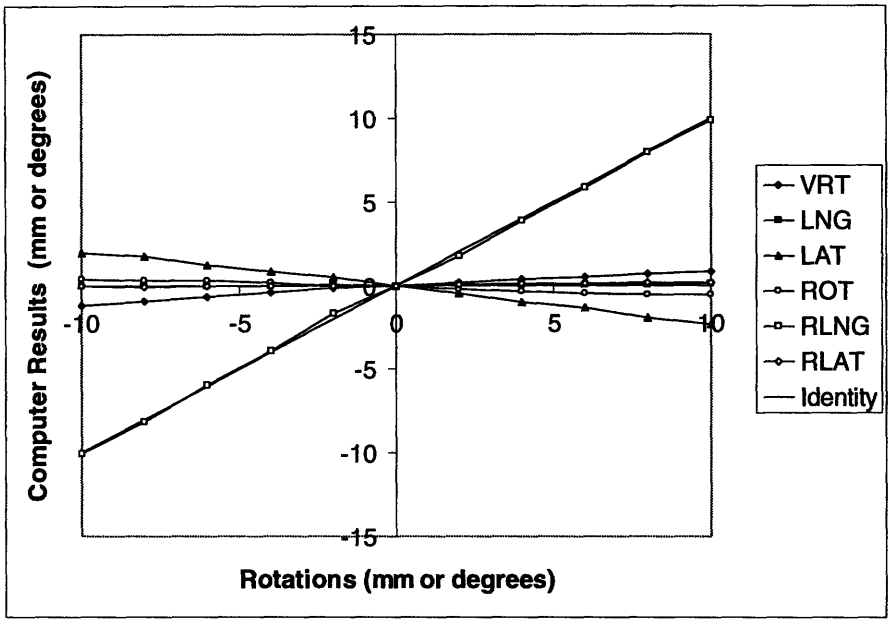

9d

Figure 9 (a-d): Graphs showing AlignRT results from a movement in a single direction. Note: rotations and translations are compiled into one graph despite units difference, they are not directly comparable.

In every translation, the data became more unreliable the further away from the zero point it was. The graphs in figure 9 (a-c) were compiled from all of the usable data.

Beyond the limits in the graphs, the results found were irreproducible. Figure 9a includes the first points where the data becomes unreliable, as an example. This is why the two endpoints on that graph indicate a large, sudden increase/decrease in values. With increasing distances from zero, some points required several attempts to get consistent data. A point was deemed "out of range" if a reasonable, consistent result was not obtained after ten tries. The out of range values were inconsistent with each other as well; the results would vary widely from picture to picture, even though the phantom had not been shifted. Finally, the field of view for the mini cam was determined to be approximately 15 cm high by 15 cm wide at the focal point of the camera.

3. Error

Within the limits, bounded by unreliable data, there are several possible sources of error. The most important is a possible camera/stage misalignment. If the direction of motion of the stage and phantom were not perfectly aligned with the internal axes (created during calibration), we would see data similar to the results seen. In other words, AlignRT may record a purely longitudinal move by the stage as a vector combination of longitude and other movements. This may explain the results showing a slight movement in directions that the phantom did not move. One other source of error is that the 3 rotations the stage can undergo do no rotate about the same origin. This did not come into play in this experiment, as the only rotation was about the spine phantom (latitudinal axis), but should be taken into account for future experiments that look at intentional rotations of the stage about the other two axes. One final source of error is the inherent error in the AlignRT system. This has been previously stated as better than 0.8 mm and 0.1^{o} rms (12).

The 3D error for the 3 translations, vertical, longitudinal and latitudinal is also considered, as shown in the following figures. The 3D error was found by first finding the difference between the actual movement and the AlignRT computed movement of the phantom. Then the square root of the sum of the squares of the vertical, latitude and longitude differences gave the 3D error. In figure 10, the 3D error is plotted versus the known movement of the phantom.

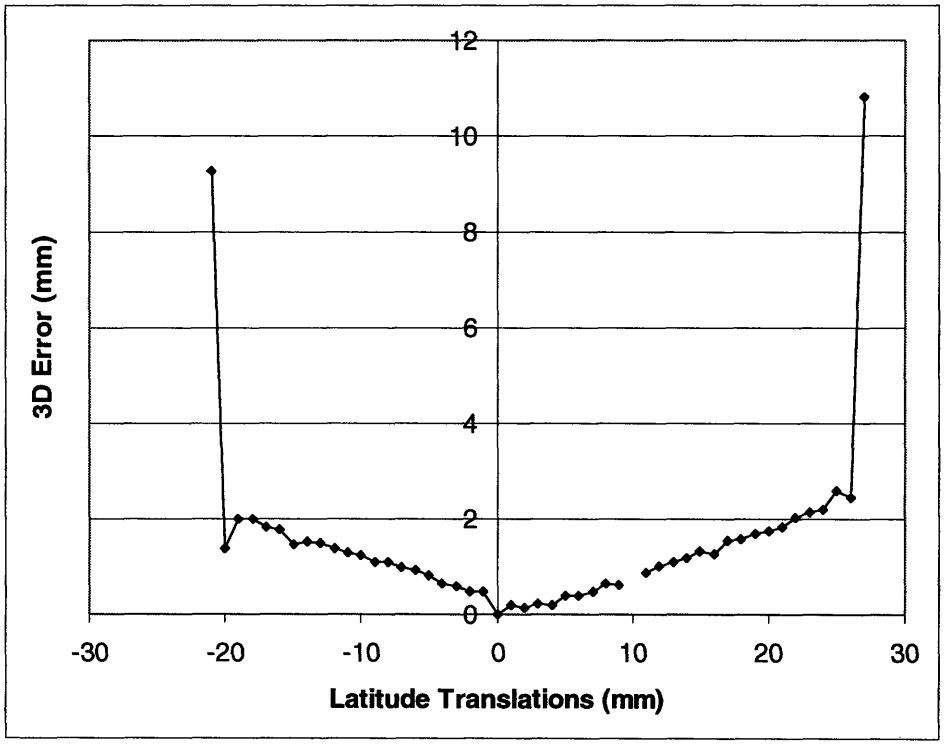

10a

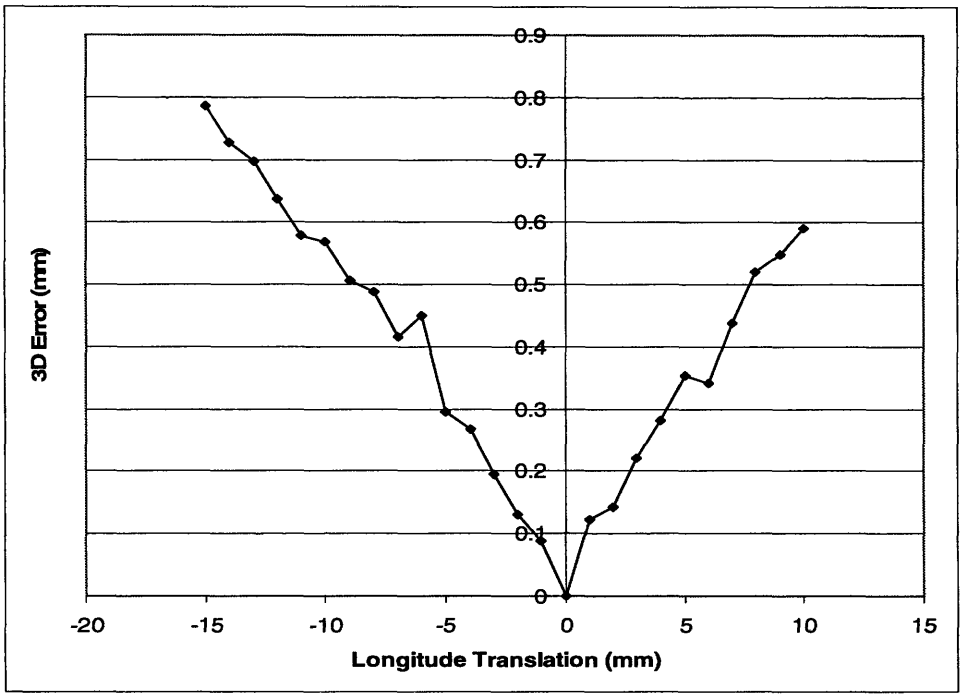

10b

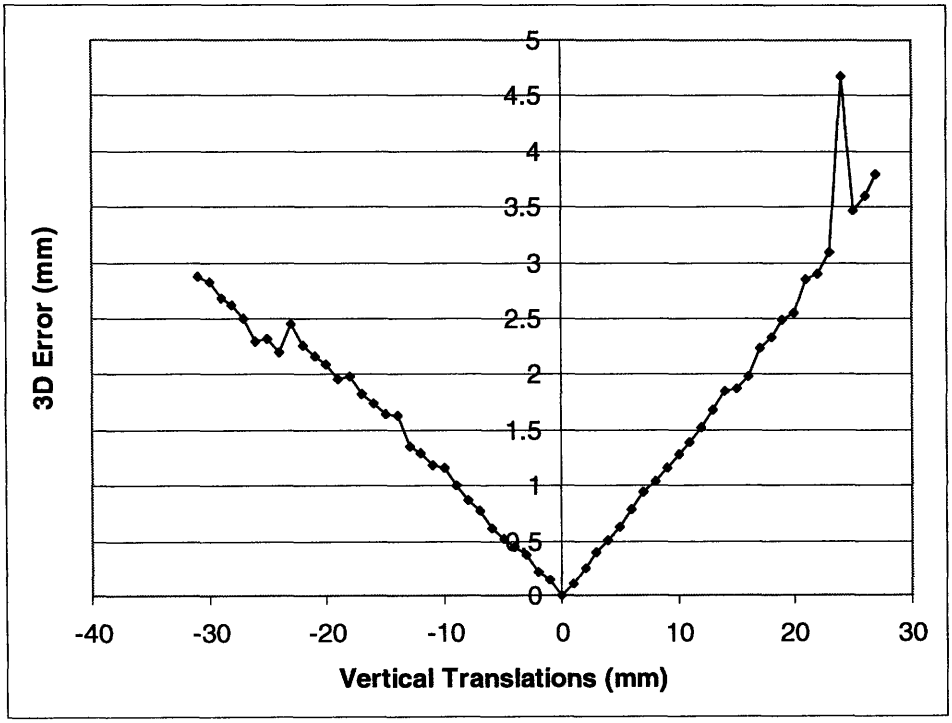

10c

Figure 10: Graphs demonstrating the 3D error for different translations.

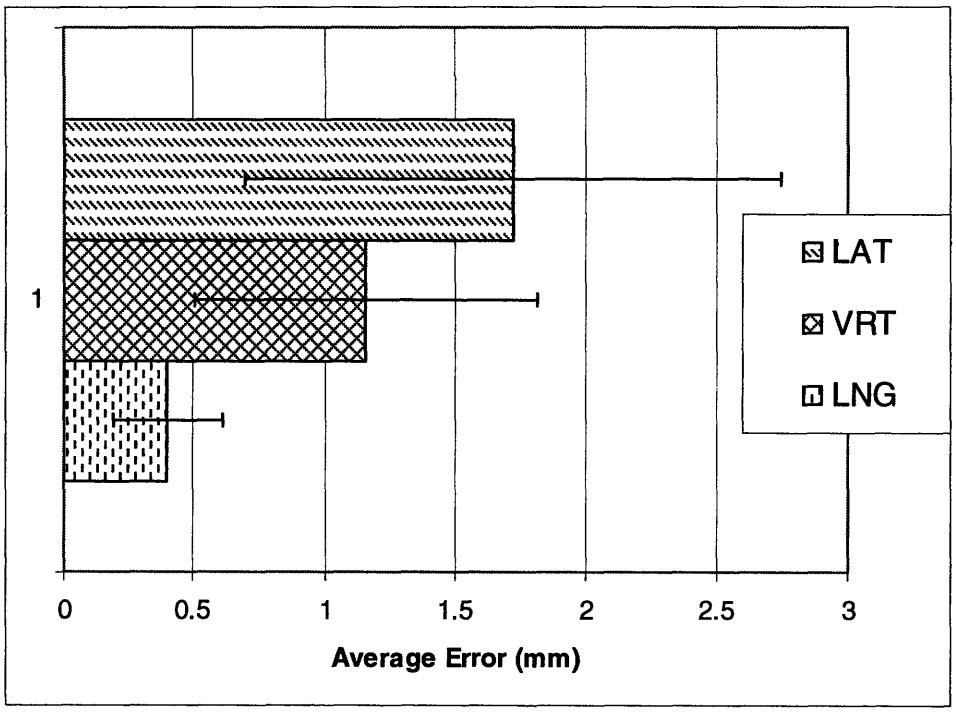

Figure 11: Graph showing the average 3D error for each direction of translation with error bars of one standard deviation.

As demonstrated in Figure 10 (a-c), a similar pattern is seen in each graph. Increasing error is seen the further away the stage is from its zero point. Again, two unreliable data points have been left in the Figure 10a to demonstrate the increased error in these points. Figure 11 shows the average error for each direction of movement with error bars indicating one standard deviation plus or minus the value. The average error is greatest for the vertical direction and smallest for the longitudinal direction. Though the error gets larger as the stage moves away from zero, it was observed that the image quality from the AlignRT program remained consistently high from the zero point until the data became unreliable.

4. Discussion

This analysis highlighted some of the problems that should be considered when using the Mini Cam. First, the camera has quite a small field of view at only about 15 cm

square at the focal point. This could severely limit the applications this camera could be used for. The camera seemed to only handle a misalignment of 2.5-5.5 cm, depending in which direction the misalignment was. Outside of this range the data became unreliable and irreproducible. The camera was also quite difficult to calibrate. First, it was difficult to find a place for the calibration plate where all of the calibration dots could be seen by the camera. Also, it was impossible to calibrate with the plate perfectly vertical with respect to the camera. This caused the camera's flash to reflect onto the shiny surface of the plate which blanched out the calibration dots, making it too difficult for the computer to analyze. As the location of the calibration plate determines the internal axes of the program, being unable to calibrate vertically makes it hard to correctly line up the camera axes with the axes of motion of the mechanical stage. Since the error seen in this analysis increases with increasing displacement, it is reasonable to assume that once the axes were properly aligned, much of this error would vanish. On the positive side, this camera is portable and it is possible to calibrate once and then move the camera to different locations to image.

IV. Deformation Analysis

1. Methods

In order to study the deformation of the breast over the course of a patients' treatment, AlignRT images were taken during the treatment (treatment image). The treatment surface is also referred to as the surface map for treatment or SMT. A surface was also reconstructed from a CT scan taken about 1-2 weeks before the treatments began (CT image). A comparison was then done between the CT image and each treatment image and between the first day's treatment image (SMT1) and each subsequent treatment image. Two separate references were used so that the deformation could be studied over the 2-3 week period covering the CT scan through the radiation treatments and over just the course of the treatment.

Each comparison of images was aligned with the AlignRT program. The images were aligned so that deformation could be examined without concern that the results were due to setup error. The program gave shifts for both 4 and 6 degrees of freedom, allowing for different styles of couches. Unless otherwise specified, assume the image and data is from a 6 degree of freedom calculation. The 3D images were then run through Matlab (Mathworks Inc.) using a program written by Marco Riboldi, which shifts the image the amount and direction suggested by AlignRT. The CT surfaces were also run through this program to shift the CT image's center to the treatment isocenter based on data found during the treatment planning. The images were then run through the VTK program which compared the two surfaces, point by point. It returned a color wash image visually representing the distance between the surfaces and a list of the distances between points across the surface, limited by an input region of interest. That list was then run through

Matlab to create a histogram of the distances between points on each surface. From the histogram, the absolute mean and the standard deviation of points was recorded. These values represented the average and standard deviation of the distance between the two surfaces over the entire region of interest. For each patient the data was aggregated to find an average and standard deviation of the absolute mean and standard deviations. The data was then combined for all patients and the average and standard deviations found. A total of 20 patients were used to study breast deformation.

2. Truncation

During this investigation, it was discovered that the data that formed the histogram needed to be truncated to exclude irrelevant data. Often with the CT comparisons it was found that there were occasional single values that were far outside the spread of points, and therefore were most likely erroneous data. The values of these points were not clinically expected. One possible cause is due to the fact that the CT surfaces are not true surface images, merely a collection of contours that represent a surface generated from axial CT slices with a slice thickness of 1 – 2.5 mm. If the program is comparing a point which does not exist on the anterior side of the CT image, it may then find a corresponding point on the posterior side, or the couch, depending on how the CT was constructed. After analyzing many histograms, a truncation point of ± 20 mm was decided. It was a point that was far outside of the full spread of data points, but cut off the irrelevant data. Figure 12 shows the small number of isolated extraneous points on either side of the main spread. The section from -50 to -100 mm was chosen for a close up as it had a higher concentration of these points.

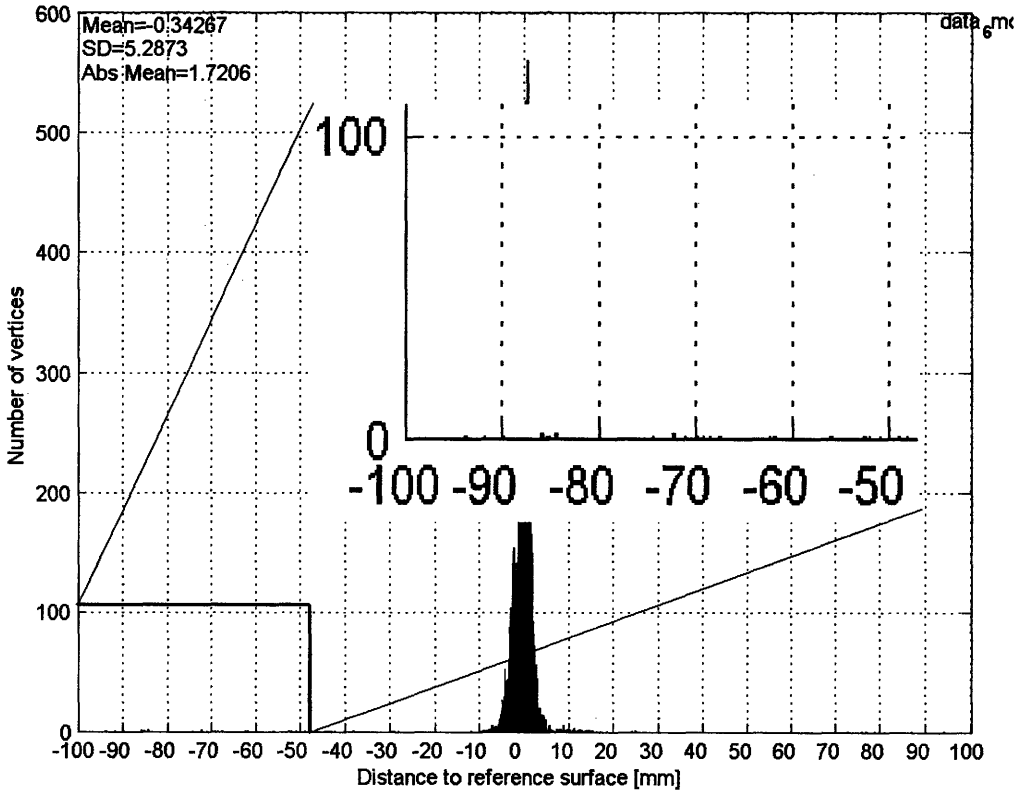

Figure 12: Image from patient 30 showing the small number of erroneous data points that were truncated.

3. Results

Overall, the results were positive. Deformation was not significant for the majority of cases. The deformation was much greater in the CT comparison, with a greater elapsed time between images, than the 1st day's image comparison. This is also due to breathing. It is an issue in the CT surface because the CT couch is translated through the scanner as the patient is breathing, so ripple artifacts are formed in the CT surface. This information can be seen in the color wash representation and the histograms. More deformation is represented by different colors on the image and a wider distribution on the histogram.

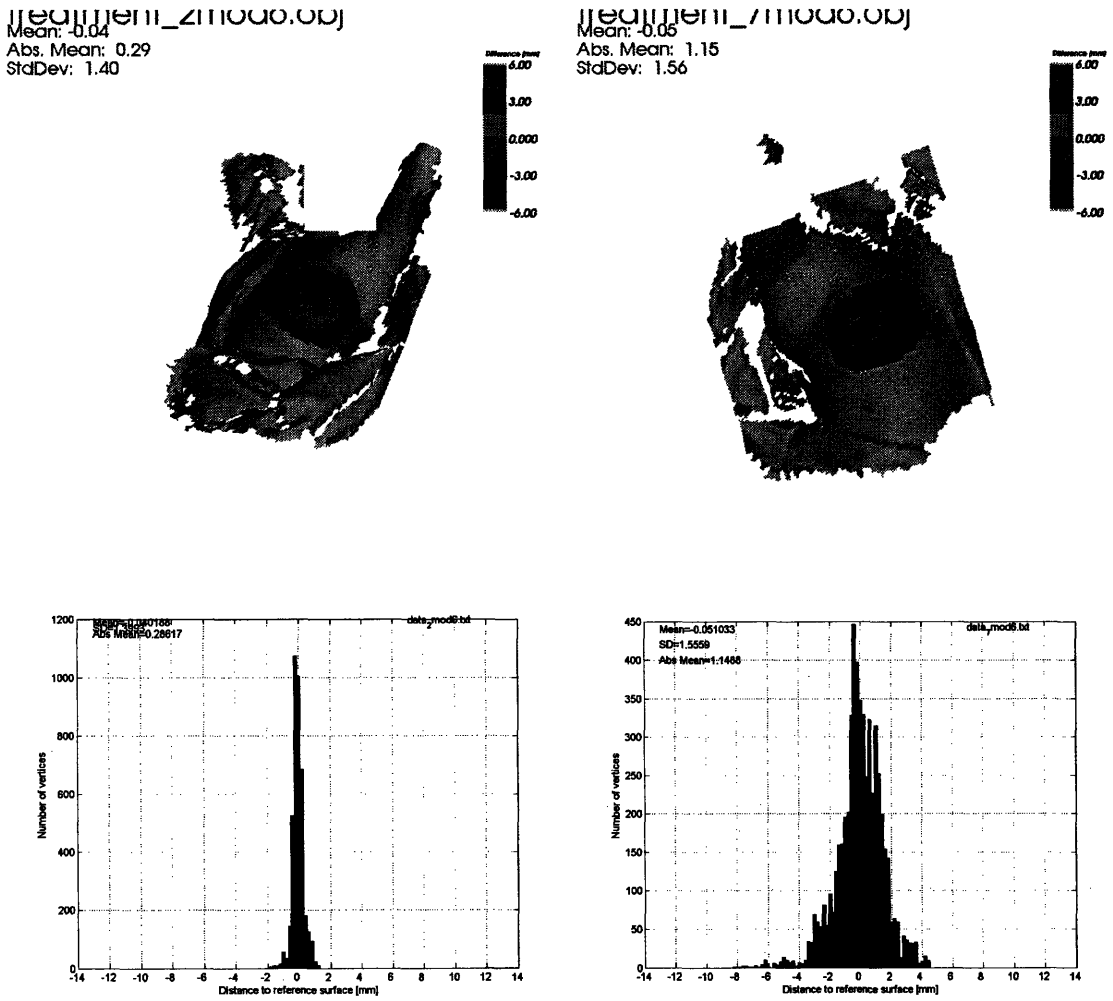

Figure 13: Images and histograms showing an example of little deformation (left, patient 21) and much deformation (right, patient 18) for a first treatment image to each subsequent treatment image comparison.

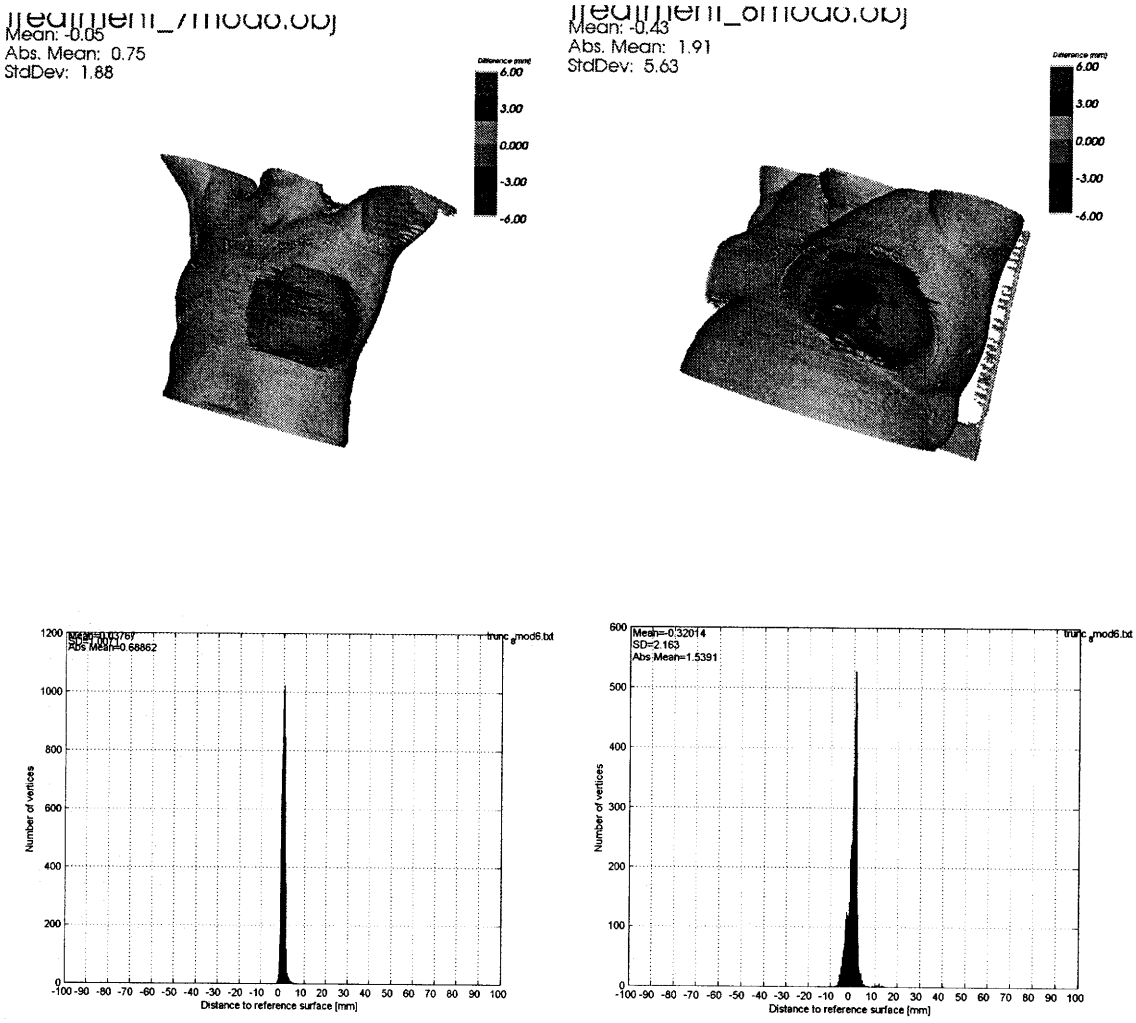

Figure 14: Images and histograms showing an example of little deformation (left, patient 7) and much deformation (right, patient 30) for CT image to treatment image comparison.

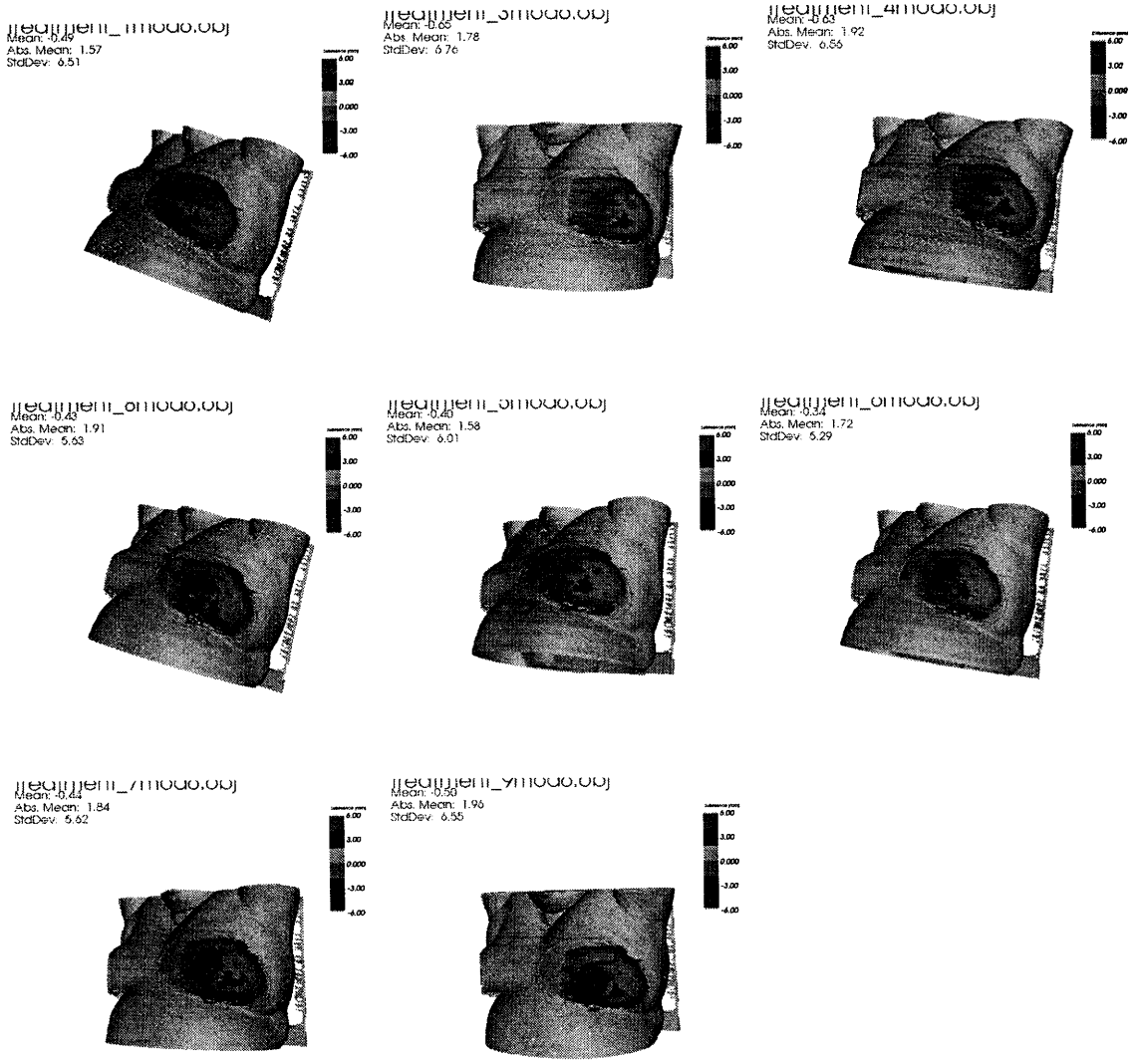

Figure 15: Series of images, one for each treatment, demonstrating the deformation for patient 30 over time, for a CT image to each treatment image comparison.

Table 1: Table giving the average and standard deviations in millimeters over all patients for the distances between two surfaces. The range of data is also shown.

	Avg Standard Deviation	Error (Standard Deviation)	Avg Absolute Mean	Error (Absolute Mean)
CT Comparison				
Average	1.489	0.185	1.099	0.137
Standard Deviation	0.436	0.071	0.301	0.061
High Values	2.321	0.325	1.703	0.311
Low Values	0.831	0.062	0.619	0.049
SMT1 Comparison				
Average	0.741	0.221	0.574	0.165
Standard Deviation	0.235	0.125	0.190	0.111
High Values	1.210	0.487	0.967	0.421
Low Values	0.386	0.069	0.299	0.063

Figure 16 compares the average standard deviation (Avg St Dev) and average absolute mean (Avg Abs Mean) versus the PTV or the breast volume of the patients. The average absolute mean and average standard deviation values were found by averaging, over all of the treatments for a patient, the absolute mean and standard deviation values found using the VTK software described earlier. No correlation was found between the breast volume or planning treatment volume and the average or standard deviation of histogram points for each patient (see Figure 16).

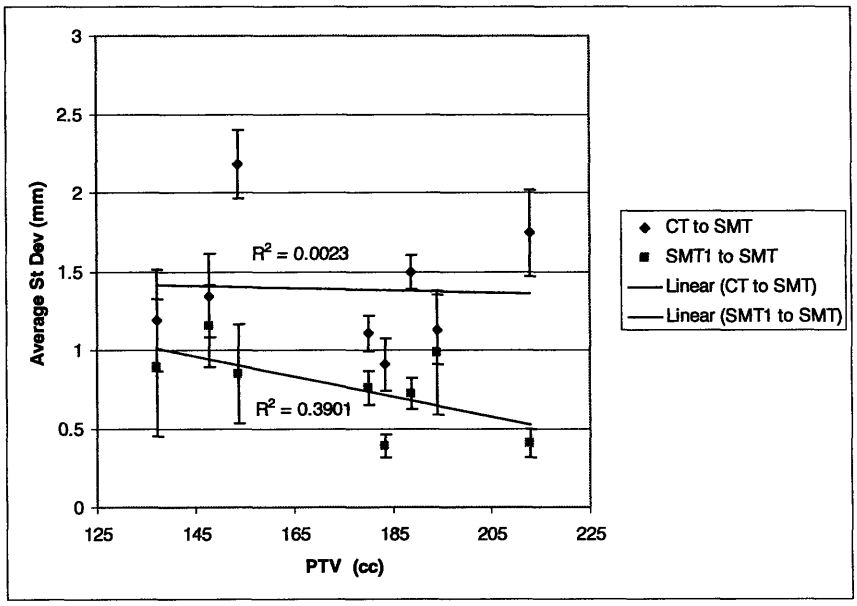
Average St Dev (mm)
3
2.5
2
1.5
1
0.5
0
125
145
165
185
205
225
PTV (cc)
R² = 0.0023
R² = 0.3901
CT to SMT
SMT1 to SMT
Linear (CT to SMT)
Linear (SMT1 to SMT)

16a

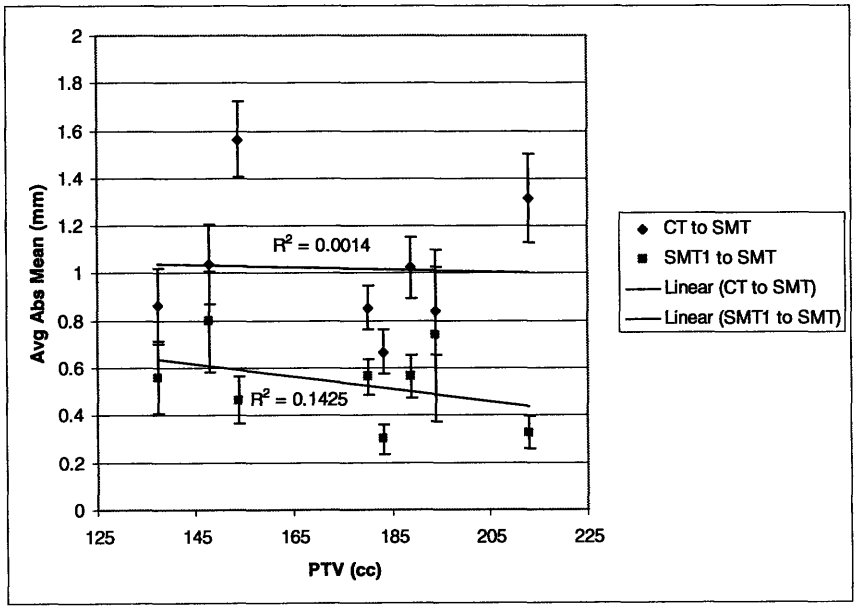
Avg Abs Mean (mm)
2
1.8
1.6
1.4
1.2
1
0.8
0.6
0.4
0.2
0
125
145
165
185
205
225
PTV (cc)
R² = 0.0014
R² = 0.1425
CT to SMT
SMT1 to SMT
Linear (CT to SMT)
Linear (SMT1 to SMT)

16b

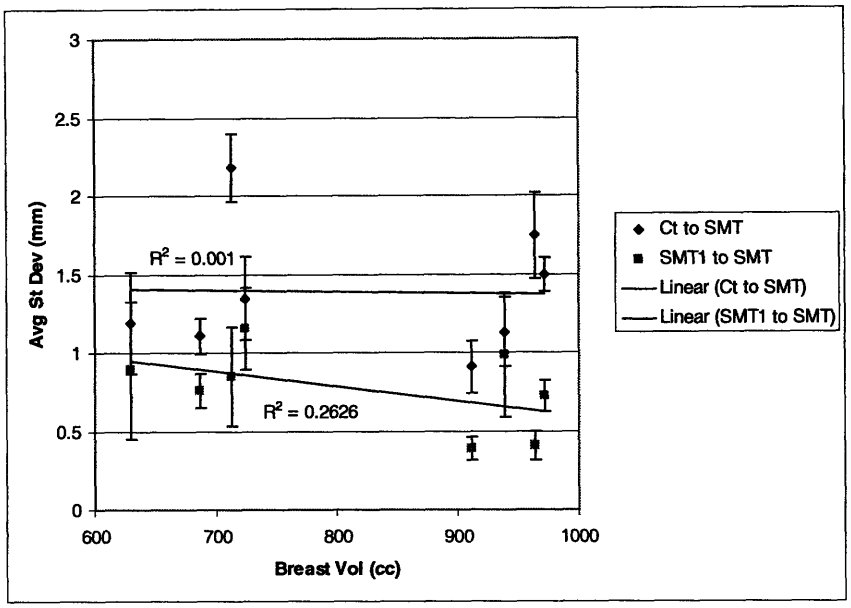

16c

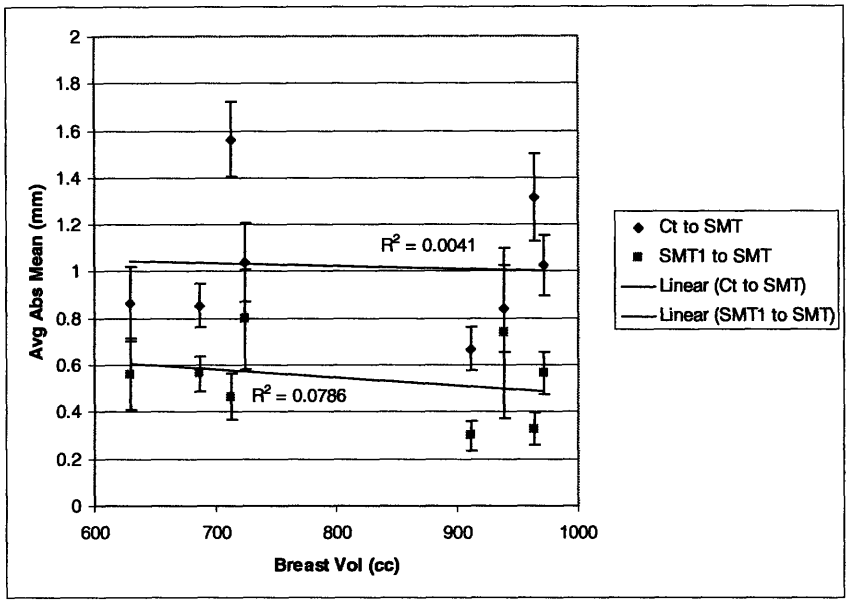

16d

Figure 16: Graphs showing comparisons between breast volume, PTV and standard deviation and average for the histogram values for both comparisons.

Some images demonstrated the need for a 6 degree of freedom (DOF) couch in the clinic. See figure 17 for an extreme example of how the ability to do rotation in 3 directions improved the alignment of the patient.

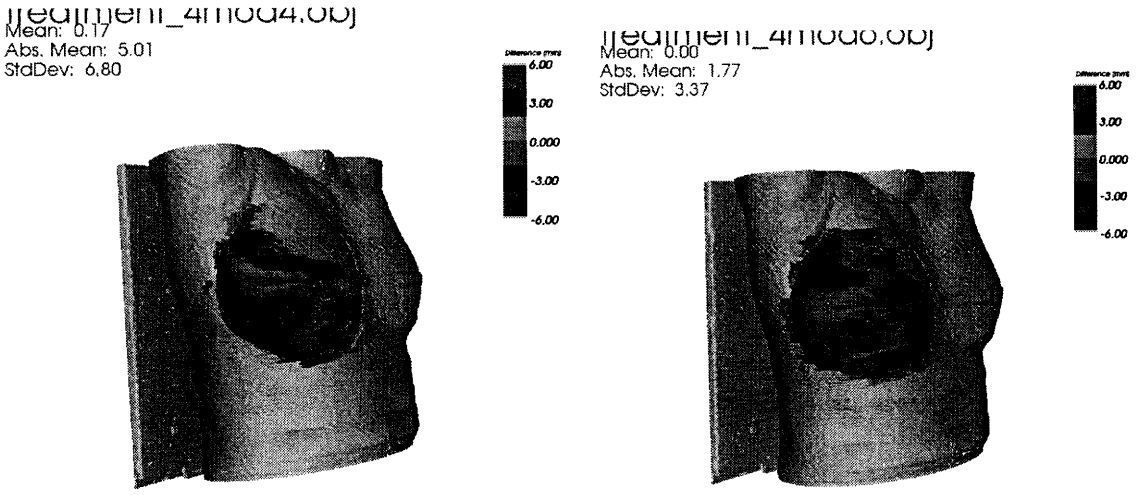

Figure 17: An example of rotation of the breast in 4 DOF (left) and 6 DOF (right).

4. Error

The most likely cause for erroneous results is due to breathing. The ripples seen on the CT surfaces represent the amount of breathing present (larger ripples means deeper breaths). This can cause the deformation to appear larger than life if the patient was at a different point on the breathing cycle when the images were taken, because the breathing could add millimeters difference onto the site of deformation.

5. Discussion

Overall, the deformation was not very large or prevalent, especially for the first treatment image to subsequent treatment image comparisons. The average absolute mean never exceeded 2 mm for any patient in the CT comparison and 1 mm for the SMT1 comparison. The average is nearly twice as large for the CT comparison versus the first treatment comparison. This is most likely due to the fact that the time difference between treatments was no more than 4 days, whereas the time difference between the CT image and the treatment images could be weeks. Breathing must also be taken into consideration

and will be discussed in a later chapter. When looking at the series of images from the same patient it is interesting to note how the spots of deformation increase and decrease over time. In many of the cases, the site of deformation happened at the lumpectomy site, possibly indicating swelling or sinking directly caused by the surgery. Another issue that was noticed was the possibility of a rotation of the patient (Figure 17) that was not accounted for in the 4 DOF simulation. It can be seen that allowing for all 6 DOF clears up many of the discrepancies seen in the 4 DOF image. Overall, no correlation was found between breast or PTV and essentially the amount of deformation seen. This is an interesting result as it is often assumed that deformation and surface changes become larger as breast size increases.

V. Breathing Analysis

1. Methods

Breathing is an important consideration when studying surface alignment. It is important to know how much breathing could move the breast and therefore the tumor site. In order to study this, AlignRT's gating function was used. This program took images of the patient on the couch for 10 seconds with a frame rate of 7.5 frames per second. A trace was created for each ten second movie, taken as close to the isocenter as possible so that the movement would closely mimic the movement of the tumor. The trace was automatically normalized by the gating program so that the lowest point of the sample was zero height. The image data was extracted at several trace points (5-10 points) and analyzed separately. At each trace point chosen for further analysis, the surface image was extracted and compared with the surface image taken at the lowest (exhale) point on the trace. The previously mentioned VTK program, written by Marco Riboldi and Christoph Bert, was used to compare the images. The program returned a list of the distances, in millimeters, for each point on the surface in the region of interest. Matlab was then used to create a histogram of this data, containing the absolute mean and standard deviation of the distances. This data was then plotted, along with the trace for each ten second breathing sample. Basically this comparison gave the average rise of an area (the ROI) versus the rise over a single point that the trace showed. The highest rise, or peak, from breathing (inhale) was recorded for each sample and then compared to the peak values for the same patient and for the different patients.

Respiratory gating is when radiation treatment is only done at certain points of the breathing cycle. As the inside of torso, and the tumor, moves with the inhale/exhale of the

lungs, a more accurate targeting of the tumor is achieved. Conventional methods, usually used for lung or abdomen patients, involve placing a marker on the abdomen of the patient which triggers the radiation to be on only during a pre-specified portion of the breathing cycle (16).

The difference in peak to peak breathing motion was compared between a point on the breast and a point on the abdomen for one patient. As the conventional method of respiratory gating examines a point on the abdomen as a reference, it is unknown if this motion accurately mimics the motion of the breast. This comparison will examine if this type of gating is feasible for breast radiotherapy. Of interest is the amount of motion of the breast relative to the amount of motion on the abdomen, as well as the synchrony of respiratory motion in the two regions.

Three patients were studied for the general gating section and one patient was used for a breast versus abdomen comparison. Each patient was asked to breathe normally. Images were taken during their normal radiation therapy sessions.

2. Results

The amount of peak-to-peak breathing motion (inhale to exhale) was calculated and shown in Table 2. The average and standard deviation values were computed based on the statistical analysis of the breathing trace, rather than from the VTK software. Anywhere from 2-10 samples of data was taken from each patient, where one sample refers to 75 images taken over 10 seconds. It can be seen that while the variability in breathing motion between patients is high, the peak variability within a patient's data is similar for all patients. This can be seen in the fact that the standard deviations for all

three patients are almost equivalent. Patients exhibited from one to three breathing cycles in ten seconds.

Table 2: Values showing the maximum, average and standard deviation of the peak-to-peak motion from each ten second sample for each patient.

Patient Number	Samples	Highest Breath (mm)	Ave. High Breath (mm)	St. Dev High Breath (mm)
21	5	2.4	2.16	0.33
22	10	1.7	0.99	0.36
24	2	1.9	1.65	0.35

Figures 18 and 19 show examples of 10 second breathing traces, taken from a single point on the breast surface, seen during this experiment. At selected points, the surface image was extracted and compared with the surface image of the patient at exhale or the zero point (image 17 for figure 18 and image 69 for figure 19). Points where images were extracted were chosen by selecting images at the peak, valley and intermediate points on the breathing trace. Each plot shows the absolute mean and standard deviation for the region of interest (the breast) for different points along the trace, as calculated by VTK.

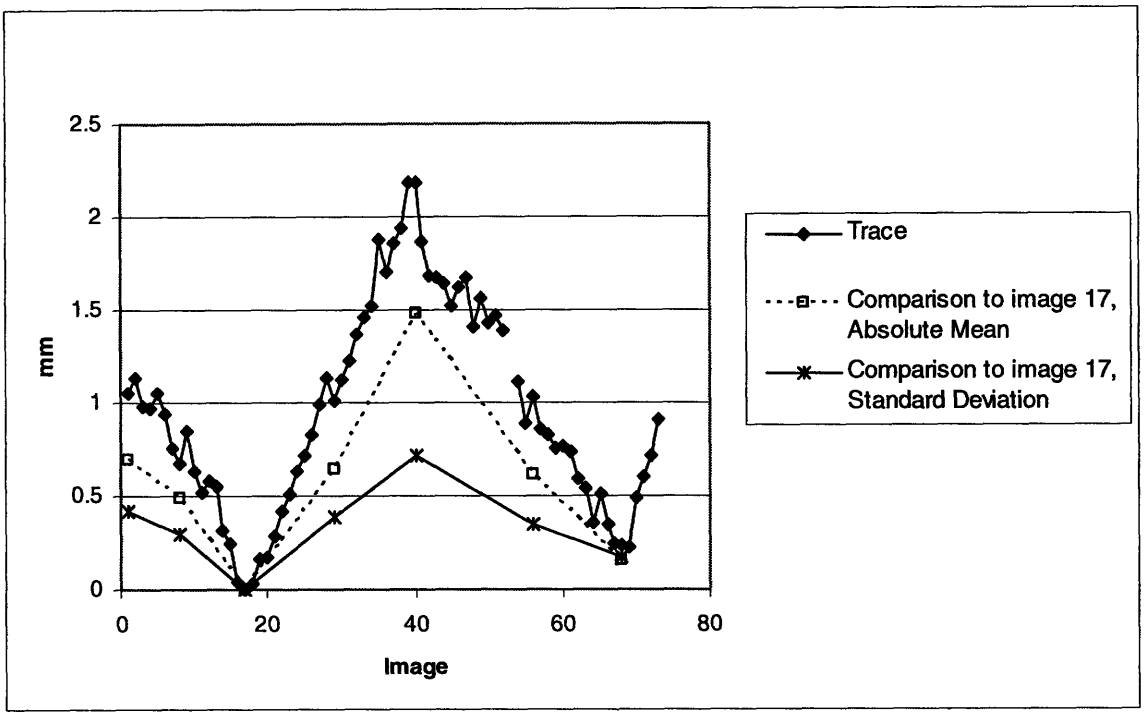

Figure 18: Trace of the movement of a single point and the absolute mean and standard deviation of the ROI for sample 5, patient 21.

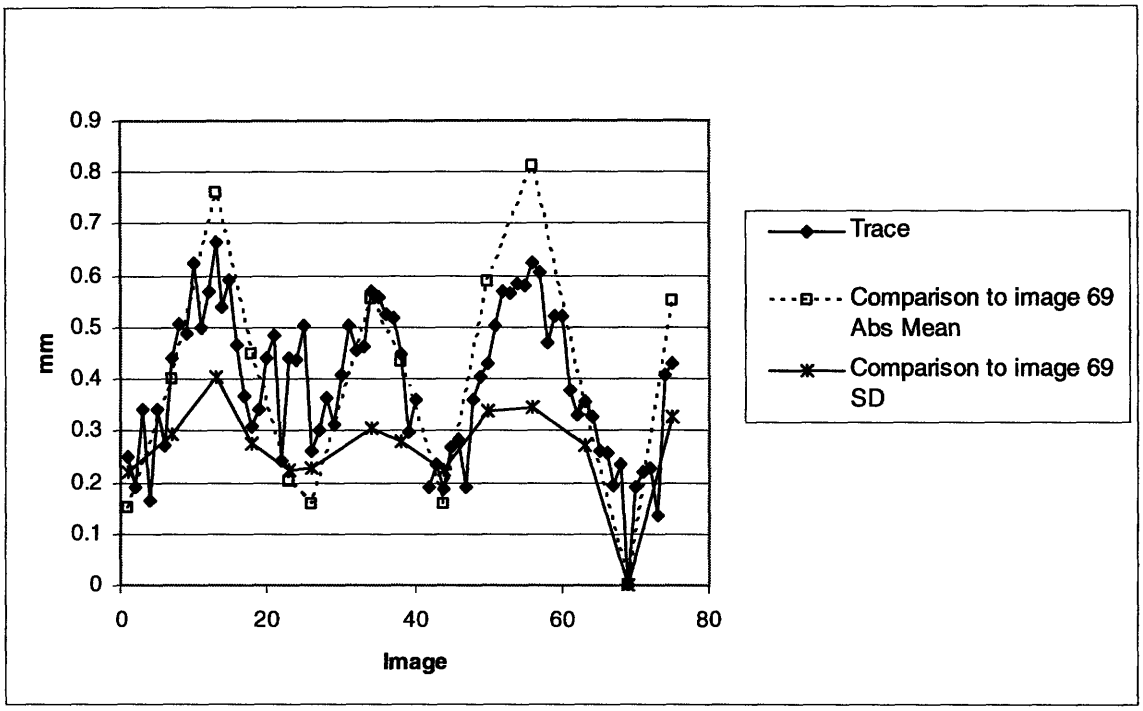

Figure 19: Trace of the movement of a single point and the absolute mean and standard deviation of the ROI for sample 7, patient 22.

Figure 20 shows the peak differences between a point selected on the breast surface and the abdomen. In general, the peak to peak breathing motion is three times greater when measured on the abdomen.

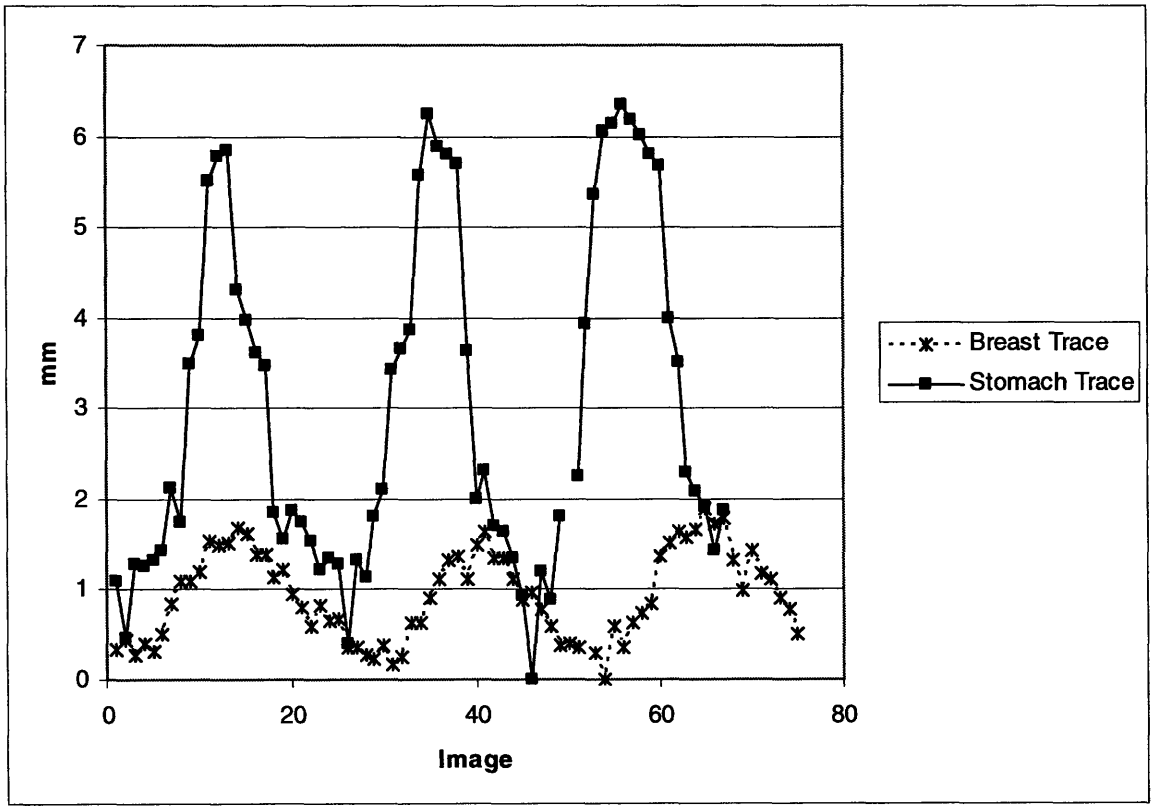

Figure 20: Comparison of the trace for a point selected on the breast versus a point on the abdomen for sample 2, patient 24.

3. Error

There was one main source of error in this study. The VisionRT software was discovered to have some variability to it, perhaps from a software bug. The program seemed to come up with a different number of trace points each time the same data was run. The program took 75 images in the 10 seconds but the trace showed anywhere from 60-74 points. Within each sample, the number of trace points had a variability of ±5 points. This means that when running the exact same data through the program, different numbers of trace points were created, sometimes finding different minimums each time.

Figure 21 is an example of data collected by running the same 75 images through the program several times and getting different results. This data was found by examining the upper abdomen of the patient, at midline. The abdomen was used to exaggerate the height difference to better visually represent the variability of the program.

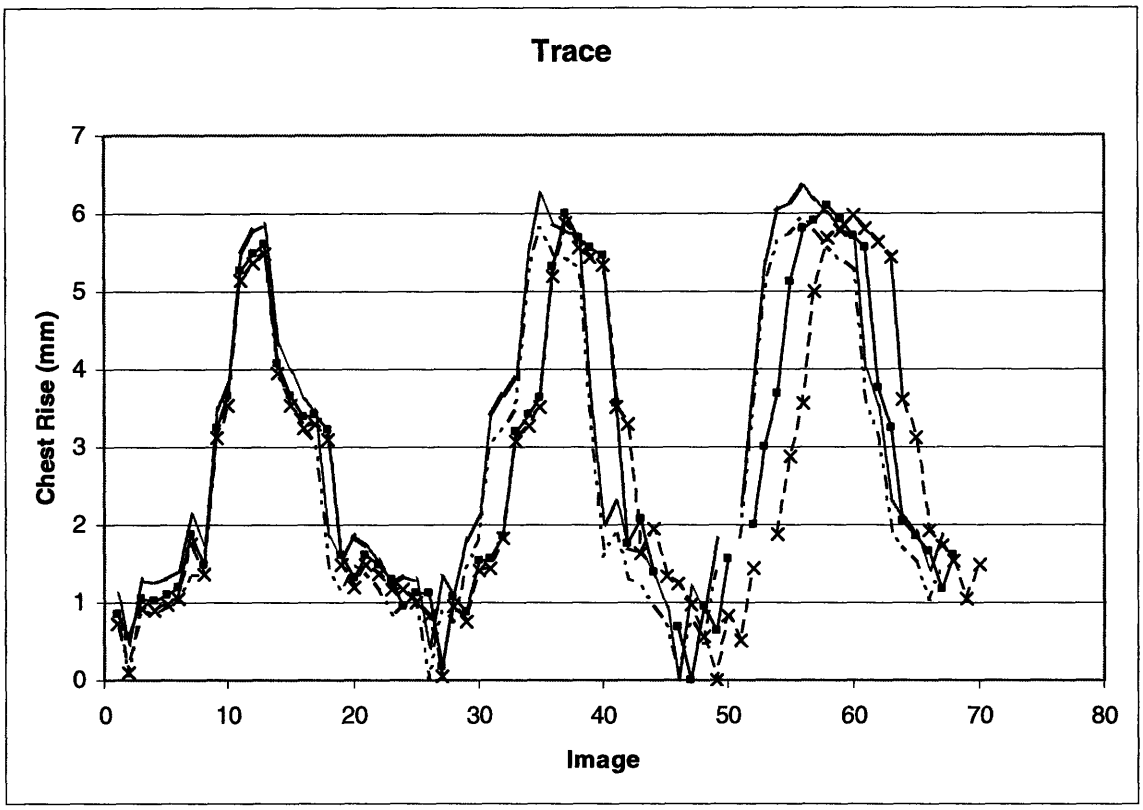

Figure 21: Four traces that are all the results of running the same data through the AlignRT software.

It can be seen from Figure 21 that the 4 different traces are all almost exactly the same at the beginning, but spread out as the trace continues. This seems to demonstrate an error in the programming that should be solved before further study. This variability is also pronounced in Figure 20. This issue has been reported to VisionRT and is under investigation. This error is important to consider because the reference (lowest) point changes from trace to trace. This makes it difficult to choose one reference image for comparison purposes. Also, no reliable comparisons were possible between the abdomen and breast regions with this phase shift artifact.

4. Discussion

The average peak to peak breathing motion of a point as close to the isocenter as possible was seen to be 0.99-2.16 mm. Out of the three patients studied the highest amount that the breast moved was 2.4 mm. All patients exhibited a similar variability in the maximum peak to peak values of their breathing during the ten second samples. The abdomen traces were approximately three times higher than the breast traces. The spatial variability of the respiratory breathing trace should be fully understood when designing gated treatments. More patients would need to be studied to see if the amount of motion, as well as the 0.3-0.35 mm standard deviation, is accurate for a population. The AlignRT software errors found during this analysis should be rectified before further analysis is undertaken.

VI. Alignment Comparison

1. Methods

A comparison between clip and surface alignment is the goal in this section. During a patient's treatment, several alignments occurred (see figure 22). When the patient first entered the room they were aligned on the couch via lasers. A surface image, referred to as a laser image, was taken at this point, at exhale. The therapist then did a clip alignment using OBI. The OBI system first took an x-ray of the patient on the couch, at exhale. The therapist then matched up the radio opaque clips at the tumor site in the x-ray to the DRR. The OBI software then calculated the couch shifts needed to align the patient to the DRR via clip location. The shifts recommended were recorded and carried out. Treatment was begun. Another surface image was taken, referred to as the treatment image (SMT), at exhale. The first radiotherapy session's treatment image is referred to as SMT1. For this section of the study, eight patients were used. Unless otherwise noted, all data refers to a 6 degree of freedom comparison.

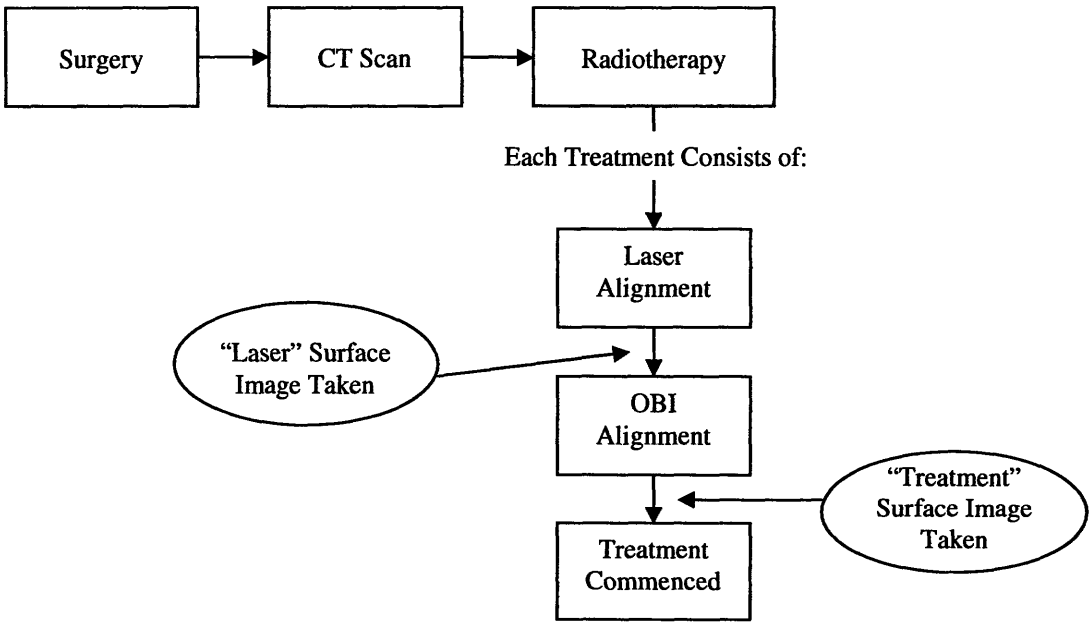

Figure 22: Flowchart of the processes a patient undergoes during treatment.

A set of five comparisons were carried out: CT reference (surface image created from CT scan) compared with each laser image (CT to Laser), CT reference compared with each treatment image (CT to SMT), 1st treatment image compared with each laser image (SMT1 to Laser), 1st treatment image compared with each subsequent treatment image (SMT1 to SMT) and each laser image compared with that day's treatment image (Laser to SMT).

The CT to Laser comparison demonstrates the accuracy of the laser alignment of the patient, assuming the CT alignment is correct. The CT should be consistent with the DRR since the DRR is created from the CT scan. The DRR is what the OBI software uses to align the patients. The CT to Laser comparison gives the difference between the CT scan surface and the patient surface after laser alignment. Ideally, these results match the OBI shifts if the CT location is taken to be accurate and the patient is moved by the OBI shifts to reach the correct treatment position. The CT to SMT comparison tells the accuracy of the CT positioning, assuming the clips are ground truth. For each treatment, the difference between the surfaces should be zero because the treatment position was found by aligning to the DRR created from the CT scan. They should be identically placed, assuming consistent alignment with OBI. The SMT1 to Laser comparison looks at the shift between the surface from the first treatment position, assumed correct, and each subsequent laser setup. These shifts should match the OBI shifts, assuming that SMT1 is accurate and matches that day's treatment image, because the therapist moves the patient by the OBI shifts to attain the (assumed) correct treatment position. The SMT1 to SMT gives the difference of the treatment positions from day to day. Ideally this is zero, as the treatment position should be identical each day. The Laser to SMT

shows the shift each day before the OBI shifts and after. Therefore, these results should match the OBI shifts.

Table 3: Comparison definition reference table

Comparison Name	Meaning
CT to SMT	Each daily treatment surface is compared to the CT surface created 1-2 weeks prior to radiotherapy
CT to Laser	Each daily laser surface is compared to the CT surface created 1-2 weeks prior to radiotherapy
SMT1 to SMT	Each daily treatment surface is compared to treatment surface taken at the first radiotherapy session
SMT1 to Laser	Each daily laser surface is compared to treatment surface taken at the first radiotherapy session
Laser to SMT	Each daily treatment surface is compared to that day's laser surface

Images were aligned using the AlignRT software to find the recommended shifts for each set of images. The shifts were recorded and analyzed. The 3D error was calculated for each treatment, as well as the average and standard deviation of the 3D error for each patient. The laser setup error was also calculated. The error values were compared with breast volume and planning target volume to look for correlations. The differences between the recommended shift for the CT to Laser, SMT1 to Laser and Laser to SMT comparisons and the OBI shifts for each treatment was calculated. Finally the average shifts recommended for each of the three translations (vertical, latitude, longitude), for each of the comparisons was calculated for each patient. The discussion section will examine why each of these calculations is meaningful.

2. Results

The recommended shifts for each translation for each comparison were recorded. See Figures 23 and 24 for a visual comparison of the recommended shifts with the OBI shifts for patient 21. Vertical (VRT) represents anterior/posterior shifts, lateral (LAT) represents left/right shifts and longitudinal (LNG) represents superior/inferior shifts in the

patient coordinate system. Figures 23 and 24 are representative of the data found for all patients.

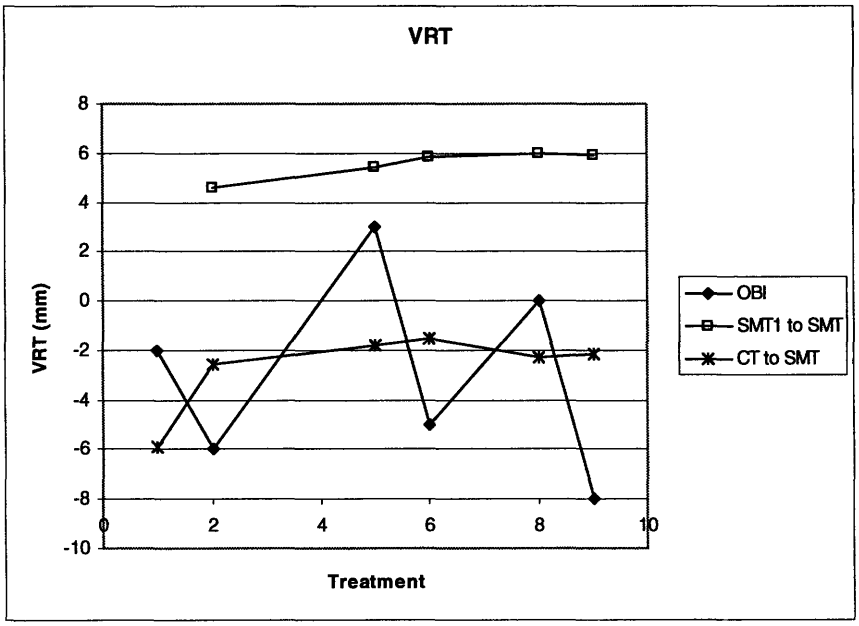

23 a

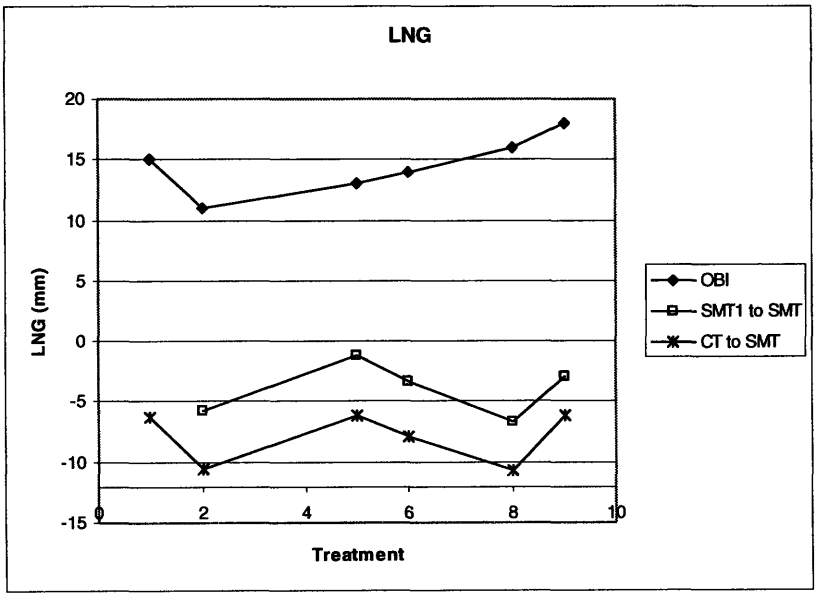

23 b

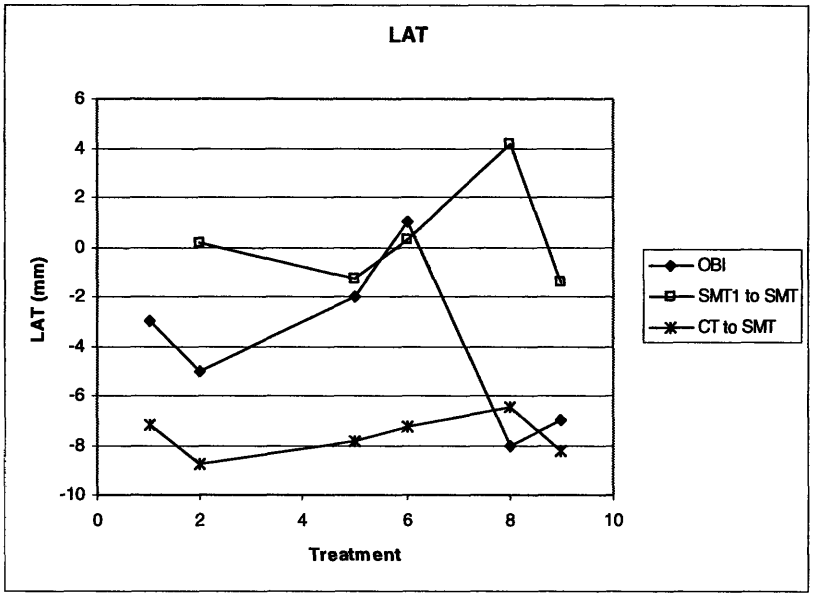

23 c

Figure 23: Comparison between the recommended shifts for OBI, SMT1 to each later treatment image and CT to each treatment image for patient 21.

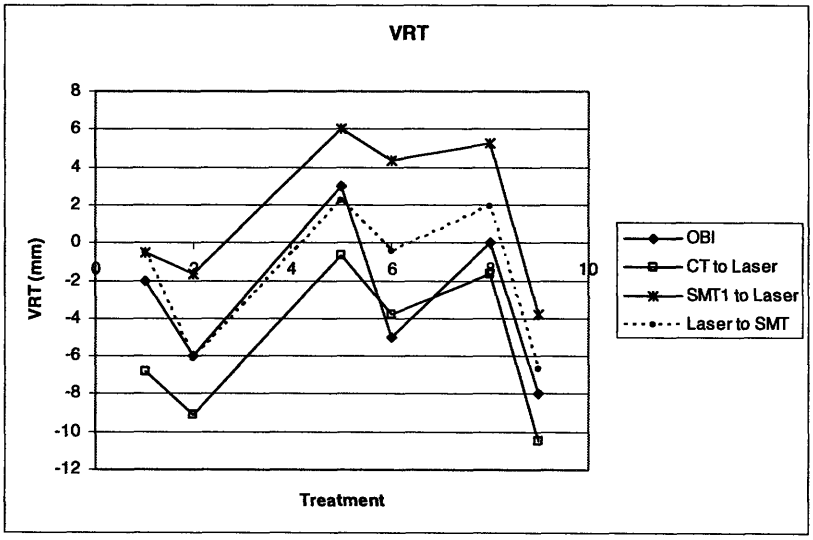

24 a

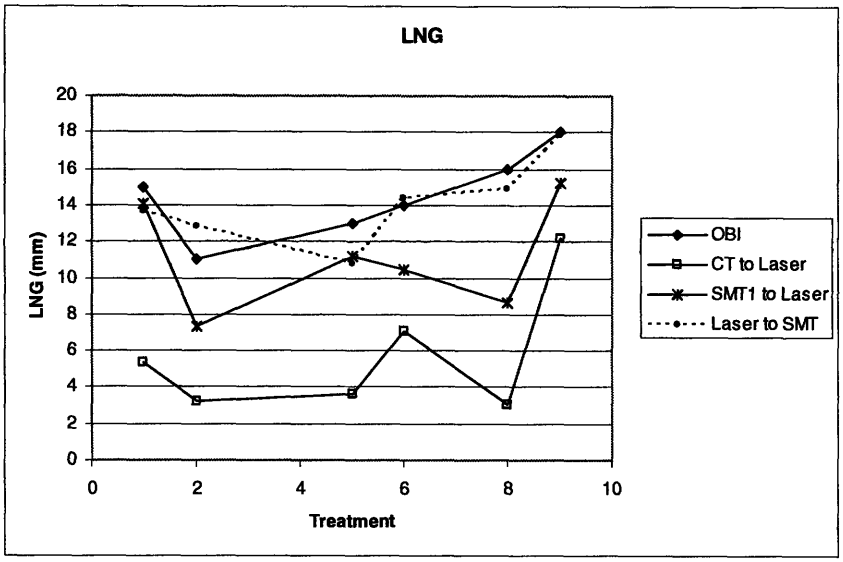

24 b

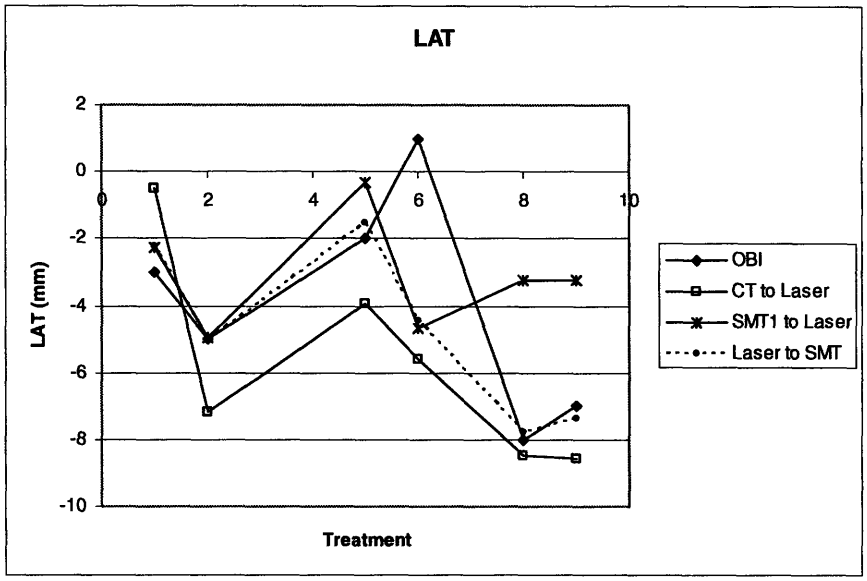

24 c

Figure 24: Comparison between the recommended shifts for OBI, SMT1 to each laser image, CT to each laser image and each laser image to treatment image for patient 21.

As seen in Figure 24, it was typical for all patients that the CT to SMT and the SMT1 to SMT comparisons followed similar patterns. It also seen that in most of the comparisons, as seen in Figure 23b and 24 b, that the largest separation was in the longitudinal direction. This was also typical of all patients. The CT to Laser, SMT1 to

Laser and Laser to SMT comparisons all generally matched the OBI curve in shape for all patients (Figure 24).

Table 4 shows the combined results of the average and standard deviation of the shifts for each comparison for each patient. Figures 25 and 26 visually represent the shifts versus breast volume and PTV. No correlation is seen. The shift values were found by averaging the 3D error values from each treatment. The shifts error represents the standard deviation of these values. Table 5 represents the OBI shifts subtracted from the shifts each of three comparisons, averaged over all treatments of a patient. The LNG values for the CT to Laser comparison are much higher than any other difference found. This appears to be systematic as the difference is always in the same direction.

Table 4: Average and standard deviation for the error for each of the five surface comparisons and the clip-based OBI shifts.

Patient	PTV (cc)	Breast Vol (cc)	OBI Shift	OBI Shift error	CT-Laser Shifts	CT-Laser Shifts error
20	137.2	630	16.38	2.22	6.28	1.74
21	153.7	713	16.02	2.64	10.54	4.33
26	194	938.7	15.54	6.78	11.49	6.35
27	183.2	911.4	14.54	1.07	5.53	1.68
25	213	963	17.23	2.09	6.99	2.96
24	180	687	17.95	2.17	6.15	2.47
18	147.9	724	13.42	1.27	3.60	1.48
22	188.7	971	20.77	6.47	16.52	7.46
Averages	174.71	817.26	16.48	3.09	8.39	3.56

Patient	SMT1-Laser Shifts	SMT1-Laser Shifts error	Laser-SMT Shifts	Laser-SMT Shifts error
20	17.12	2.95	16.74	2.91
21	12.50	2.50	15.43	3.12
26	17.92	10.28	15.01	7.77
27	12.92	4.99	15.06	1.22
25	16.02	2.42	17.59	2.60
24	16.19	2.67	19.70	2.22
18	14.92	1.27	13.45	1.04
22	25.76	6.25	20.33	6.31
Averages	16.67	4.17	16.66	3.40

Patient	SMT1-SMT Shifts	SMT1-SMT Shifts error	CT to SMT Shifts	CT to SMT Shifts error
20	2.58	1.57	14.02	1.46
21	7.29	1.57	11.54	1.49
26	6.04	1.67	10.02	1.90
27	1.75	0.71	12.44	1.19
25	4.31	1.48	18.94	1.68
24	6.20	0.91	13.90	3.73
18	4.62	1.39	13.36	0.56
22	9.45	2.70	14.44	4.12
Averages	5.28	1.50	13.58	2.02

Table 5: Individual and combined data for the each treatments' OBI shifts subtracted from the VisionRT recommended shifts for each comparison.

	CT to Laser Average Differences (4 dof)				SMT1 to Laser Average Differences (4 dof)				Laser to SMT Average Differences (4 dof)			
Patient	VRT	LNG	LAT	3D Shifts	VRT	LNG	LAT	3D Shifts	VRT	LNG	LAT	3D Shifts
20	-1.28	-11.71	-2.77	13.15	-0.29	-0.30	-2.09	5.59	1.93	-0.32	0.55	3.42
21	3.77	-8.99	-3.80	11.17	7.20	-2.78	0.12	8.46	1.49	-0.37	-0.78	2.82
26	-0.62	-13.70	0.54	14.08	1.24	0.72	-0.38	3.93	2.28	-0.75	0.34	2.65
27	-1.77	-10.70	1.70	11.05	0.02	-1.10	-1.90	3.84	1.19	0.37	-0.36	1.53
25	-2.45	-16.72	-0.19	17.20	-1.44	-0.25	3.49	4.49	1.63	0.32	0.72	2.35
24	-1.28	-15.65	0.74	15.85	-0.52	-3.53	3.04	5.25	0.50	1.33	0.83	2.58
18	1.29	-12.67	1.35	12.92	4.07	-1.62	-1.21	5.20	1.18	0.14	0.50	1.65
22	0.15	-13.07	6.44	14.81	6.05	7.73	-3.11	10.62	2.79	1.54	0.20	3.70
Average	-0.27	-12.90	0.50	13.78	2.04	-0.14	-0.25	5.92	1.62	0.28	0.25	2.59
St Dev	2.00	2.52	3.10	2.15	3.29	3.47	2.40	2.39	0.71	0.81	0.55	0.76

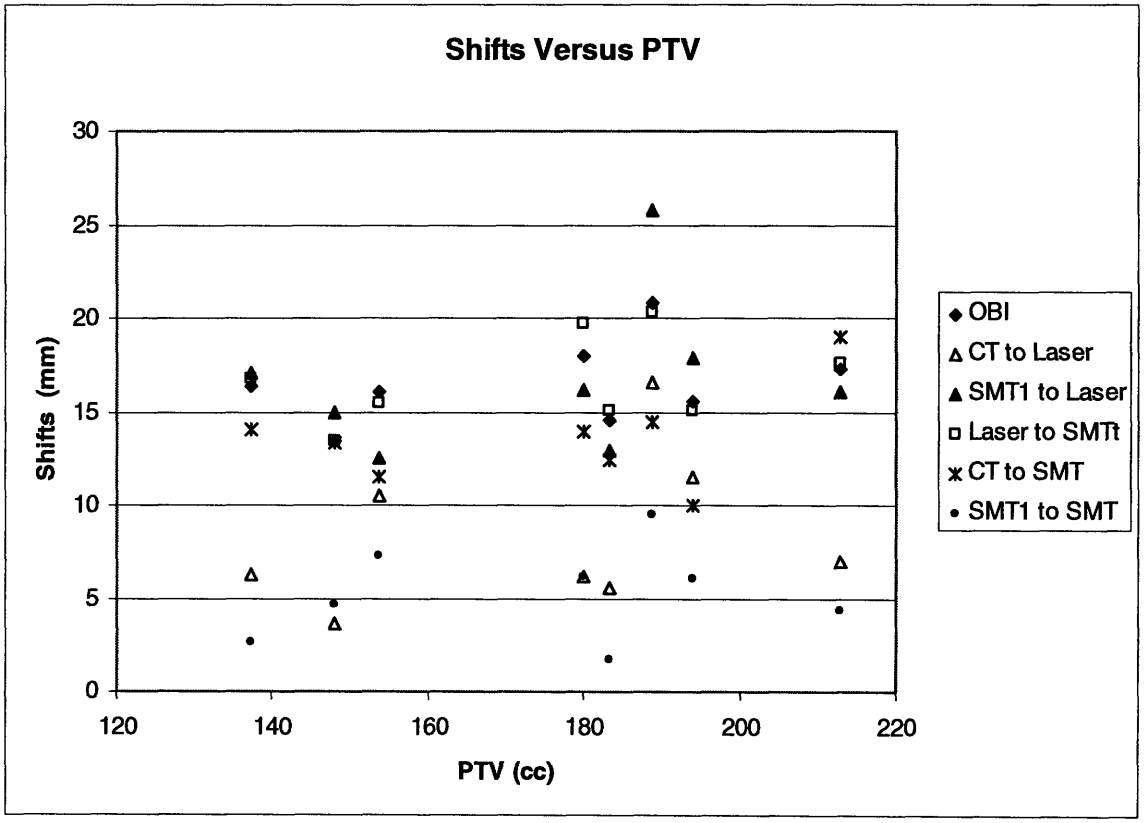

Figure 25: Figure displaying the comparisons between each patients PTV and shifts for each of 5 comparisons plus the OBI shifts.

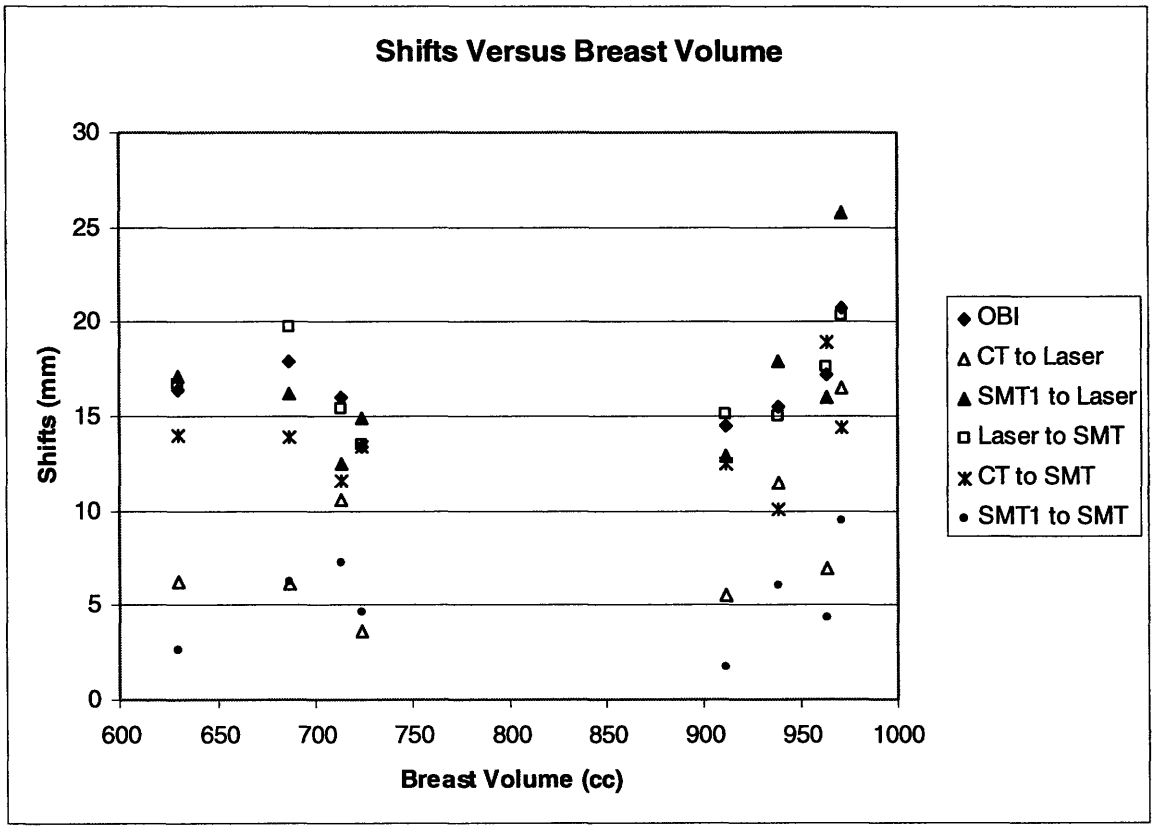

Figure 26: Figure displaying the comparisons between each patients' breast volume and shifts for each of 5 comparisons plus the OBI shifts.

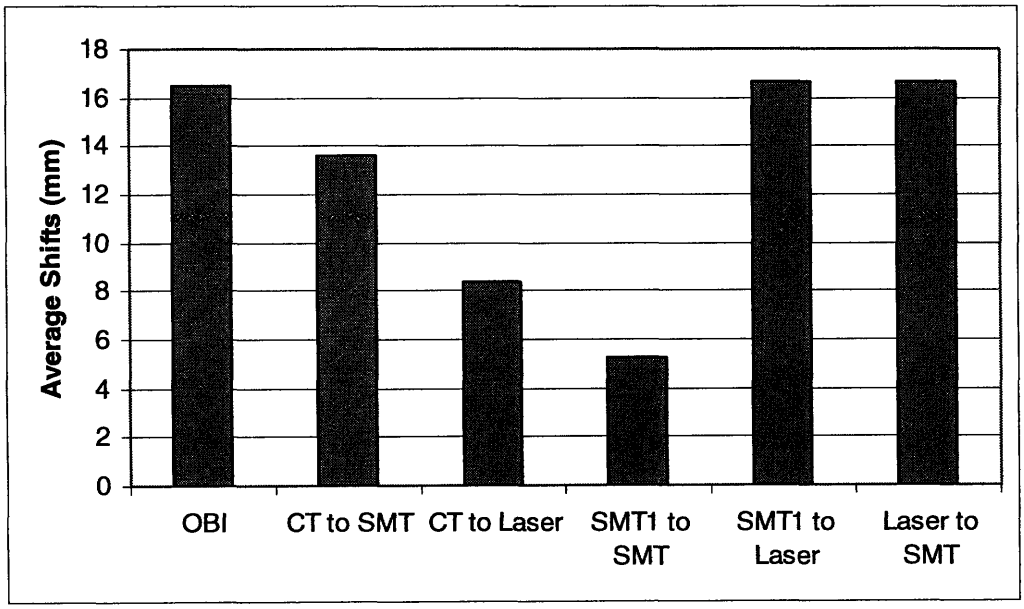

Figure 27: Figure showing the average shifts over all of the patients for each comparison.

The average shifts in each of the 3 translational directions (VRT, LAT, LNG) that were recommended for each comparison were compiled for each patient. Figure 28 displays an example of this type of graph.

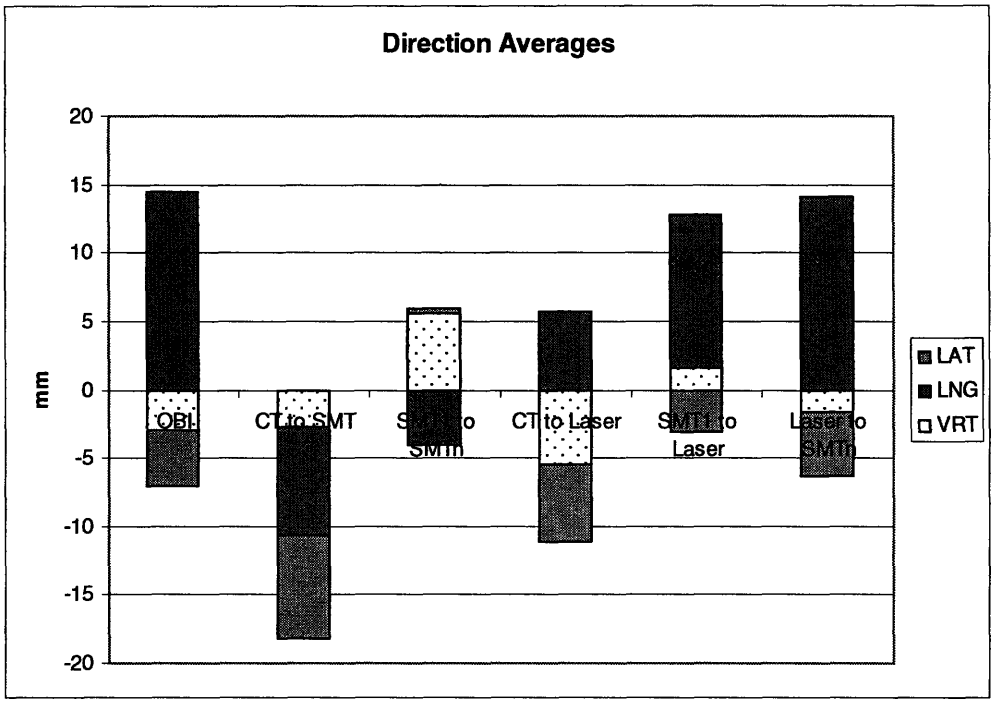

Figure 28: The average recommended shift for each translation, for each comparison, for patient 21.

3. Error

In this study, there are several possible sources of error. Human error is likely as clip alignment requires the therapist to visually line up the clips. The therapist also takes the surface images and x-ray at exhale by visually watching the patient. This could also introduce error. The magnitude of these errors is most likely a few millimeters. Clip movement could also cause error. It is unknown if clips placed at the site of a lumpectomy can move over time. If the clips are not in a constant location, their use as ground truth would cause an additional error in this analysis.

Several errors could stem from the CT scan taken of the patients before commencing radiotherapy. As the patient is translated through the scanner while breathing, ripple artifacts are formed in the CT surface. This could hinder the alignment process. This process may also introduce error into the DRR that is used in the OBI comparison. Occasionally a patient had trouble fitting into the CT bore in the same position as they would be later placed in the treatment room. This may cause changes in the position of the patient which could affect both the CT surface and the DRR.

4. Discussion

The average OBI shift was found to be 16.48 mm. The average shift values of SMT1 to Laser, Laser to SMT and CT to Laser were expected to be similar to the OBI shifts and were 16.66 mm, 16.67 mm and 8.39 mm respectively. The average shift values of CT to SMT and SMT1 to SMT were expected to be zero and were 13.58 mm and 5.28 mm, respectively. The CT to SMT comparisons and the SMT1 to SMT comparisons followed similar patterns in most patients. The fact that the SMT1 to SMT comparison was often closer to zero than the CT to SMT comparison indicates that the patient treatment positions were more consistent compared with the first treatment than with the CT surface. However, the variation from each treatment from the first treatment was still approximately 5 mm. This was a bit larger than expected.

From patient to patient and from treatment to treatment there was no clear comparison (CT to Laser, SMT1 to Laser, and Laser to SMT) that was consistently closest to the OBI shifts. Generally speaking, they matched the shape of the OBI curve. When the CT to Laser curve matches the OBI curve it means that the CT surface is a good match for clip location. This means that lining up the patient to the CT surface and

lining up the patient via clips would give the same results. When the SMT1 to Laser curve matched the OBI curve, the first treatment image is an accurate model for clip placement. When the Laser to SMT curve matches the OBI curve, it means that the surface visualization is accurately measuring the amount the patient has shifted due to the OBI couch shifts. For each of these comparisons, there were some treatments that matched the OBI curve very closely and some that were far off.

Table 4 provides a numerical comparison between the different 3D errors for each shifts averaged over all treatments and directions. Under ideal conditions, the errors for the CT to SMT and SMT1 to SMT would be zero because the two surfaces compared should match up, as explained earlier. The 3D errors for CT to laser, SMT1 to laser and laser to SMT should match the OBI shifts because the alignment shifts between the surfaces are expected to be the same as the OBI shifts, also explained earlier. Figures 25 and 26 show these results visually. Table 5 shows the results when the OBI shifts for each treatment are subtracted from the VisionRT recommended shifts. Ideally, each average should be zero as each comparison should equal the OBI shifts. The results are 5.92 mm, 2.59 mm and 13.78 mm for SMT1 to Laser, Laser to SMT and CT to Laser respectively. All results appeared close to what was expected except the CT to Laser comparison, the SMT1 to Laser comparison and the CT to SMT comparisons. The CT to Laser comparison showed values far lower than the OBI shifts. They were anywhere from one third to three fourths as large as the OBI, while the other comparisons had 3D errors that were much closer to the OBI values. This means that the CT surface compared to both the laser image and SMT was not as good a method of alignment as the first treatment image. The CT to SMT shifts were twice as far from zero as the SMT1 to SMT

comparison shifts. This means that, once again, the CT reference is not as accurate as the first treatment image. Based on this data, aligning the patient using the first treatment image (SMT1) is the most accurate way of utilizing surface alignment. This method, however, requires the first day treatment position to be setup based on clips. Therefore, based on these data, the OBI system is still an integral part of patient setup for PBI.

VII. Conclusions and Future Work

1. Conclusions

The Mini Cam has many limitations, but also many benefits. It is highly portable and does not need to be calibrated at each location. This means the user can calibrate at one station and take the camera to many locations around the hospital and immediately take images. However, it does have a small field of view (15 cm by 15 cm) and an even smaller range that a surface can be misaligned (2.5 to 5.5 mm). Calibration is an important issue as the calibration creates the internal axes of the camera. If the alignment functions are to be used, the internal axes must be implicitly known so as to best interpret the suggested alignment shifts. If a use can be found where these limitations are not an issue, this camera will be extremely useful.

Deformation is seen in many patients over the course of their treatment, but rarely exceeds 5 millimeters. CT comparisons showed greater deformation than first treatment image comparisons. The average distance separating the surfaces over the breast was only 2mm for the CT comparisons and only 1mm for the first treatment image comparisons. This was most likely due to the fact that the CT had breathing artifacts and that the time difference between the images was more than twice as long, allowing more time for deformations to form.

Breathing generally accounted for only 2 mm or less of breast peak to peak breathing motion during treatment. The variability within a single patient's maximum breast movement while breathing seems consistent at approximately 0.35 millimeters. The breast was found to have peak to peak breathing motions three times less than the motions recorded on the abdomen. This means that a scaling factor must be taken into

account when using the abdomen movement as a surrogate of the movement of a breast during normal breathing. The synchrony of the breast and abdomen movements could not be studied at this time due to errors in the AlignRT software.

Surface alignment was shown to be close to the quality of clip alignment. Overall, the comparisons using the first treatment image (SMT1) as a reference were more accurate than a CT reference as a method of surface alignment. Incorporating the deformation study, the results are the same. Breathing did not cause artifacts which could lead to misalignment or an inaccurate measure of deformation.

2. Recommendations for Future Work

The Mini Cam project should be undertaken with more attempts at a good calibration. More effort needs to be made to ensure the internal axes, as set up by calibration, are the same as the axes being studied.

Deformation could be studied further by examining more patients. A possible angle for a new study would look at the deformation at more time points. Perhaps several CT scans could be taken at defined intervals between surgery and radiotherapy, in order to better understand the deformation the breast undergoes after a lumpectomy.

Comparisons could also be made when specifically asking the patients to breathe shallowly during their CT scan, or even undergo a breath-hold CT, to minimize breathing artifacts. This could affect the results for deformation and patient alignment.

The breathing study should be re-conducted using more patients. It would be interesting to find out if the variability remained around 0.35 mm when more patients are studied. Another good breathing experiment would be to do more comparisons between

the movement of the breast compared with the movement of the abdomen during breathing.

In order to get a more accurate view of patient alignment a larger patient group should be studied. Furthermore, the inaccuracy of surface alignment using CT-based surfaces should be investigated further. The future addition of a VisionRT camera in the CT scanner will allow for further study of this issue.

VIII. References

1. National Cancer Institute. www.cancer.gov

2. Baglan, K.L. (2003). Accelerated partial breast irradiation using 3D conformal radiation therapy (3D-CRT). *Int. J. Radiation Oncology Biol. Phys.*, Vol. 55(2),302–311.

3. (2006). A Randomized Phase III Study of Conventional Whole Breast Irradiation (WBI) Versus Partial Breast Irradiation (PBI) for Women with Stage 0, I, or II Breast Cancer. *American College of Radiology.*

4. Taghian, A.G., et al. (2006). Initial dosimetric experience using simple three-dimensional conformal external-beam accelerated partial-breast irradiation. *Int. J. Radiation Oncology Biol. Phys* , 64(4), 1092–1099.

5. Major, T., et al. (2006). Dosimetric comparisons between high dose rate interstitial and MammoSite balloon brachytherapy for breast cancer. *Radiother Oncol.*, 79(3), 321-8.

6. Weed, D.W., et al. (2004). The validity of surgical clips as a radiographic surrogate for the lumpectomy cavity in image guided accelerated partial breast irradiation. *Int. J. Radiation Oncology Biol. Phys.*, 60(2), 484–492.

7. Islam, M., et al (2006). Patient dose from kilovoltage cone beam computed tomography imaging in radiation therapy. *Medical Physics*, 33(6), 1573-1582.

8. Jaffray, D.A., et al. (2002). Flat-panel cone-beam computed tomography for image-guided radiation therapy. *Int. J. Radiation Oncology Biol. Phys.*, 53(5), 1337–1349.

9. McBain, C.A., et al. (2006). X-ray volumetric imaging in image-guided radiotherapy: the new standard in on-treatment imaging. *Int. J. Radiation Oncology Biol. Phys.* 64(2), 625–634.

10. Le'tourneaua, D. (2005). Cone-beam-CT guided radiation therapy: technical implementation. *Radiotherapy and Oncology,* 75, 279-286.

11. Bert, C., et al. (2006). Clinical experience with a 3D surface patient setup system for alignment of partial-breast irradiation patients. *Int. J. Radiation Oncology Biol. Phys.,* 64(4), 1265–1274.

12. Bert, C., et al. (2005). A phantom evaluation of a stereo-vision surface imaging system for radiotherapy patient setup. *Medical Physics*, 32(9), 2753-2762.

13. Vision RT. http://ww.visionrt.com

14. Visualization Toolkit. http://www.vtk.org

15. Delaney, T.F. (2003). Intraoperative dural irradiation by customized [192]Iridium and [90]Yttrium brachytherapy plaques. *Int. J. Radiation Oncology Biol. Phys*, 57(1), 239-245 .

16. Varian Medial Systems. http://www.varian.com